NUCLEAR OVERHAUSER EFFECT AND CROSS-RELAXATION RATE DETERMINATIONS OF DIHEDRAL AND TRANSANNULAR INTERPROTON DISTANCES IN THE DECAPEPTIDE TYROCIDINE A

MEI-CHANG KUO AND WILLIAM A. GIBBONS, *Department of Biochemistry, College of Agricultural and Life Sciences, University of Wisconsin-Madison, Madison, Wisconsin 53706 U.S.A.*

ABSTRACT The following interproton distances are reported for the decapeptide tyrocidine A in solution: (*a*) $r(\phi)$ distances between NH(i) and Hα(i), (*b*) $r(\psi)$ distances between NH(i + 1) and Hα(i), (*c*) $r(\phi\psi)$ distances between NH(i + 1) and NH(i), (*d*) NH$\leftrightarrow$NH transannular distances, (*e*) H$\alpha\leftrightarrow$Hα transannular distances, (*f*) $r\chi^1$ distances between *H*α and Hβ protons, (*g*) NH(i)$\leftrightarrow$Hβ(i) distances, (*h*) NH(i + 1)$\leftrightarrow$Hβ(i) distances, (*i*) carboxamide-backbone protons and carboxamide-side chain proton distances, (*j*) side chain proton-side chain proton distances. The procedures for distance calculations were: NOE ratios and calibration distances, σ ratios and calibration distances, and correlation times and σ parameters. The cross-relaxation parameters were obtained from the product, say, of NOE 1$\rightarrow$2 and the monoselective relaxation rate of proton 2; the NOEs were measured by NOE difference spectroscopy. The data are consistent with a type I β-turn/ type II′ β-turn/ approximately antiparallel β-pleated sheet conformation of tyrocidine A in solution and the NOEs, cross-relaxation parameters, and interproton distances serve as distinguishing criteria for β-turn and β-pleated sheet conformations. It should be borne in mind that measurement of only $r\phi$ and $r\psi$ distances for a decapeptide only defines the (ϕ, ψ)-space in terms of 4^{10} possible conformations; the distances *b–j* served to reduce the degeneracy in possible (ϕ, ψ)-space to one tyrocidine A conformation. The latter conformation is consistent with that derived from scalar coupling constants, hydrogen bonding studies, and proton-chromophore distance measurement, and closely resembles the conformation of gramicidin S.

INTRODUCTION

The nuclear Overhauser effect (1) and selective proton relaxation rates (1, 2) are now being extensively used to study amino acid (2, 3) and peptide (4–12) conformational dynamics. Cross-relaxation effects on proton relaxation rates in proteins have been reported (13, 14, 15). Glickson et al. (8) have observed that dipolar mechanisms dominate the NOEs in peptides such as gramicidin S and valinomycin, and the evaluation of interproton distances (6, 9, 10) and correlation times (9, 10, 11) from NOEs and cross-relaxation rates have appeared.

Previous NOE and cross-relaxation studies have utilized only the measurement of $r\phi$ or $r\psi$ distances between backbone protons, and claims have been made (4, 5, 6, 9, 10, 11) that these distances delineate β-turn or antiparallel β-pleated sheet conformations. This was an oversimplification because in general each interproton distance ($r\phi$ or $r\psi$) corresponds to two ϕ and two ψ dihedral angles, and hence to four possible conformations per residue. Thus for the $i + 1$ and $i + 2$ residues of a β-turn the NOE-derived $r\phi$ and $r\psi$ distances can correspond to 16 possible conformations.

Here we report $r\phi$, $r\psi$, $r\chi$ interproton distance determinations from NOEs and proton relaxation rates and the use of these to delineate (*a*) the possible (ϕ, ψ) and χ space and (*b*) the microenvironment (within 4 Å) of a given proton. In addition, by evaluating transannular and chain folding NOEs and cross-relaxation rates (σ) we demonstrate that it is possible to accurately determine the secondary conformation of a polypeptide.

The conformation proposed for tyrocidine A contains an antiparallel β-pleated moiety with a type I and type II′ β-turn at each end. Our data provides not only $r\phi$ and $r\psi$ criteria for β-turns and antiparallel β-pleated sheets but also additional criteria such as transannular and chain folding NOEs not previously reported.

EXPERIMENTAL PROCEDURE

The samples contained 4.5 mg tyrocidine A in 0.3 ml of 100% DMSO-d_6 (Aldrich). Samples were thoroughly deoxygenated, and all NOE and spin-lattice relaxation time measurements were performed on a Bruker WH-270 spectrometer equipped with a Nicolet 1180 computer. NOE difference spectra were obtained by subtraction of two spectra taken in the HG mode of the spectrometer. Typically a 2-s irradiation of a given multiplet preceded a 90° pulse; the off-resonance spectra were taken with the decoupling frequency, f_2, ~300 Hz away from the multiplet being saturated. Each of the on-resonance and off-resonance spectra represents the sum of four sets of 1,000 scans. A $(180°\text{-}\tau\text{-}90°\text{-}T)_n$ pulse sequence was used to measure the spin-lattice relaxation rates; the nonselective 180° pulse was typically 20 μs and the selective one, provided by the decoupling channel, was 10 ms.

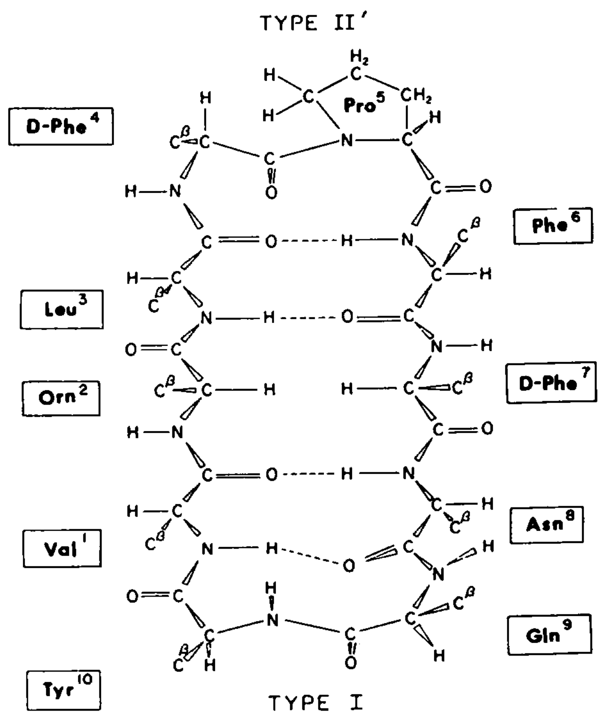

FIGURE 1 Proposed tyrocidine A conformation.

RESULTS

The amide, alpha, and beta proton assignments of tyrocidine A, in both dimethylsulfoxide and methanol, have been reported (12, 16, 17). The secondary conformation in both these solvents has been proposed (18) (Fig. 1). An analysis of the side chain region of the proton nmr spectrum established the χ^1 side chain conformations of each residue, the χ^2 conformations of the aromatic and asparagine residues and the χ^1, χ^2, χ^3, and χ^4 conformations of proline (17).

It has been shown that NOEDS (4) can be used to delineate $r\phi$ and $r\psi$ interproton distances (9, 10) either alone or in combination with selective excitation proton spin-lattice relaxation rates. The theory behind these calculations has been described (1, 2, 9) and the nomenclature used is shown.

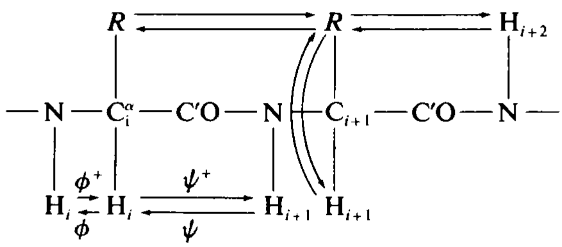

In additions to $r\phi$ and $r\psi$ distances, it will be shown here that NOEs can be used to measure $r\chi$ distances, chain folding distances between pairs of alpha protons or pairs of amide protons, and backbone and side chain proton distances.

Delineation of Proton Microenvironments by NOEDS

For a rigid molecule with a single correlation time, irradiation of a single proton gives rise to NOEs of different intensity at all protons within 4 Å, the proton microenvironment. The magnitudes of these NOEs are related to the molecular correlation time, interproton distance and the relaxation rate of the observed proton.

Fig. 2 *A* and *B* are the off-resonance (control) spectrum (*A*) and the same spectrum (*B*) with the single isolated multiplet of Gln^{9}Hα saturated. The observed NOEs in the NOEDS Fig. 2 *C* are negative. The largest negative peak is the saturated proton multiplet; on each side of both the off-resonance and decoupling frequencies are intensity changes due to partial saturation of other multiplets by the nonmonochromatic decoupling fields. The expected intraresidue NOEs are negative and located at the Hβ (χNOE) and NH (ϕ^- NOE) multiplets of Gln^9. Interresidue NOEs are of low intensity (<1%) indicating the essentially isolated nature of Gln^{9}Hα.

A more complicated, but still understandable, example is seen in Fig. 2 *D* which is the NOEDS obtained by saturating the D-Phe^4 and Tyr^{10} alpha protons. Partial saturation of resonances adjacent to the f_2 fields are more obvious than in Fig. 2 *C*. Intraresidue χ^1 and ϕ^- NOEs are observed for both D-Phe^4 and Tyr^{10} as well as interresidue NOEs at Pro^{5}Hδ1 and Hδ2 (from Phe^{4}Hα). The ψ^+ NOE for Tyr^{10}Hα is <1% but NOEs between the α, δ, and ϵ protons were found.

The proton microenvironments of the alpha protons of Phe^6 and Asn^8 can be discerned in

FIGURE 2 NOE difference spectra of tyrocidine A in DMSO-d_6; the arrows in each spectrum indicate the position of the decoupling frequence, f_2. No NOEs at the Phe ring protons or CH_3 protons are considered although they undoubtedly exist. This is due to the difficulty in distinguishing NOEs from incomplete cancellation of these intense peaks. Arrows, ↑ and ↓, refer to off-resonance and saturating f_2 frequencies, respectively. Partial saturation of multiplets close to the f_2 fields are marked with an x. (*A*) Control spectrum with decoupler off-resonance. (*B*) Spectrum with Gln^9*H*α saturated. (*C*) NOE difference spectrum (NOEDS) between *A* and *B*. The largest negative peak of one proton intensity corresponds to Gln^{9}Hα. Negative NOEs at Tyr^{10}NH, Gln^{9}NH, and Hβ are observed. (*D*) NOEDS with f_2 centered at the overlapping D-Phe^{4}Hα and Tyr^{10}Hα multiplets. NOEs are seen at Pro^{5}Hδ1 and Hδ2, Phe^{4}Hβ, Tyr^{10}Hβ, Tyr^{10}NH, D-Phe^{4}NH, Tyr^{10}Hδ, and Hϵ. (*E*) NOEDS with f_2 centered at the Phe^{6}Hα and Asn^{8}Hα multiplets. NOEs are observed at Asn^{8}Hβ1 and Hβ2, Phe^{6}Hβ, Gln^{9}NH, Asn^{8}NH, D-Phe^{7}NH. NOEs at Orn^{2}NH and Phe^{4}NH are due to decoupler power spill-over (see F). (*F*) NOEDS with f_2 centered at Val^{1}Hα and Leu^{3}Hα. NOEs are observed at the β protons of Val^1, Leu^3, and at the amide protons of Orn^2 and D-Phe^7. (*G*) NOEDS with f_2 centered at Orn^{2}NH. NOEs observed at the β and γ protons of Orn^2 and at the alpha protons of D-Phe^7, Orn^2, and Leu^3. (*H*) NOEDS with f_2 centered at Leu^{3}NH. NOEs observed at the alpha protons D-Phe^7, Orn^2, and Leu^3 but the intensities differ from those in *G* as explained in the text. The intensity at the upfield Asn^8 carboxamide (marked) is due to partial saturation of the lowfield carboxamide proton.

their NOEDS, Fig. 2 *E*; both alpha protons have the same chemical shift, the usual decoupler spillover effects are seen, but large χ^1 NOEs are observed at the Phe^6 and Asn^8 beta protons. Intraresidue ϕ^- and interresidue ψ^+ NOEs to amide protons from both alpha protons are also detected.

The proton microenvironment of $Val^1H\alpha$, reflected in Fig. 2 *F*, consists of $Val^1H\beta$, Orn^2NH, and Val^1NH. Similarly, due to simultaneous irradiation of $Leu^3H\alpha$, intraresidue and interresidue NOE signals are observed at Leu^3NH, $Leu^3H\beta$, $Leu^3H\alpha$, and D-Phe^4NH. The other intensity changes in Fig. 2 *F* are due to direct decoupler spillover at the $Asn^8H\alpha$ and $Phe^6H\alpha$ and NOEs obtained by this partial saturation of the latter.

Fig. 2 *G* shows the effect of saturating Orn^2NH; apart from partial saturation of other amide protons, NOEs are observed at $Leu^3H\alpha$, $Orn^2H\alpha$, and D-$Phe^7H\alpha$. These same three alpha proton NOEs are observed when Leu^3NH is irradiated but the intensity ratios are different (Fig. 2 *H*).

ϕ and ψ NOEs have already been reported (5, 6, 10) and converted to $(r\phi, r\psi)$ distances and hence (ϕ, ψ) angles, but the other NOEs detected in this work have not been detected or

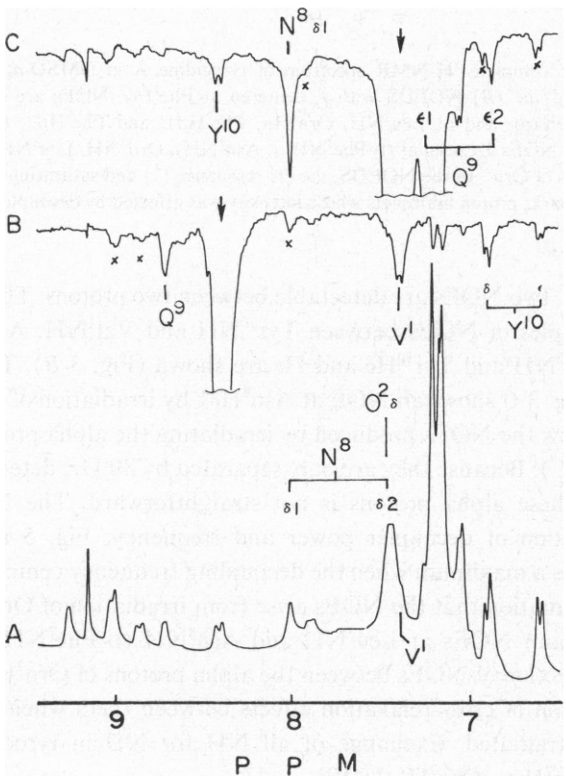

FIGURE 3 (*A*) The 270-MHz ^{1}H-NMR spectrum of the amide-aromatic proton region of tyrocidine A in DMSO-d_6 at 26°C; concentration, 15 mg/ml. (*B*) NOEDS with f_2 centered at $Tyr^{10}NH$. NOEs are observed at Val^1NH, and the δ and ϵ protons of the Tyr^{10} ring. The off-resonance frequency was centered at 10 ppm. (*C*) NOEDS with f_2 centered at three overlapping resonances, Orn^2NH_3, Val^1NH, and $Asn^8H\delta2$. NOEs are observed at $Tyr^{10}NH$ and $Asn^8H\delta1$. The off-resonance frequency was centered at 10 ppm.

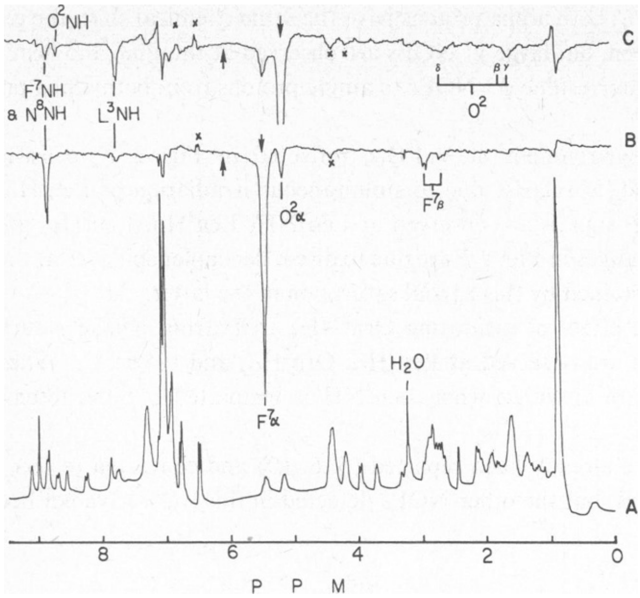

FIGURE 4 (A) The complete ^{1}H-NMR spectrum of tyrocidine A in DMSO-d_6, temperature, 26°C; concentration, 15 mg/ml. (B) NOEDS with f_2 centered at Phe^{7}Hα. NOEs are seen at Phe^{7}NH and Asn^{8}NH (which overlap), and at Leu^{3}NH, Orn^{2}Hα, Phe^{7}Hβ1, and Phe^{7}Hβ2. (C) NOEDS with f_2 centered at Orn^{2}Hα. NOEs are seen at (D-Phe^{7}NH + Asn^{8}NH), Orn^{2}NH, Leu^{3}NH, Phe^{7}Hα, and at the β, γ, and δ multiplets of Orn^2. In the NOEDS, the off-resonance (↑) and saturating (↓) f_2 frequencies are indicated and an x marks proton multiplets whose intensity was affected by decoupler spillover.

evaluated. In general, two NOEs are detectable between two protons. The NOEDS in Fig. 3 B and C contain examples of NOEs between Tyr^{10}NH and Val^{1}NH. Additional intraresidue NOEs between Tyr^{10}NH and Tyr^{10}Hδ and Hϵ are shown (Fig. 3 B). The Asn^{8}Hδ2 overlaps with Val^{1}NH and Fig. 3 C shows an NOE at Asn^{8}Hδ1 by irradiation of Asn^{8}Hδ2.

Fig. 4 A and B show the NOEs produced by irradiating the alpha protons of D-Phe^7 (Fig. 4 B) and Orn^2 (Fig. 4 C). Because they are only separated by 80 Hz, detection and quantitation of NOEs between these alpha protons is not straightforward. The NOEs were therefore measured as a function of decoupler power and frequency; Fig. 5 shows that the NOE observed at Phe^{7}Hα is a maximum when the decoupling frequency centers at Orn^{2}Hα and vice versa. Further confirmation that the NOEs arise from irradiation of Orn^{2}Hα comes from the fact that the maximum NOEs at Leu^{3}NH and Asn^{8}NH (D-Phe^{7}NH) occurs at the same frequencies. The detection of NOEs between the alpha protons of Orn^{2}Hα and D-Phe^{7}Hα was confirmed by detection of cross-relaxation effects between them when Leu^{3}NH or Asn^{8}NH (D-Phe^{7}NH) were irradiated. Exchange of all NH for ND in tyrocidine A affected the magnitude of the Orn^{2}Hα—Phe^{7}Hα NOEs.

The relaxation rates themselves qualitatively reflect the richness of the proton microenvironment. Thus the slow values $R < 2$ s^{-1} for Pro^{5}Hα and Gln^{9}Hα reflect that there are few protons available to effect relaxation in their microenvironment; for other protons ($R = 3{\sim}6$ s^{-1}) several protons are available to efficiently relax the proton in question. This conclusion is supported by the small number of NOEs obtained by irradiating Pro^{5}Hα and Gln^{9}Hα on the

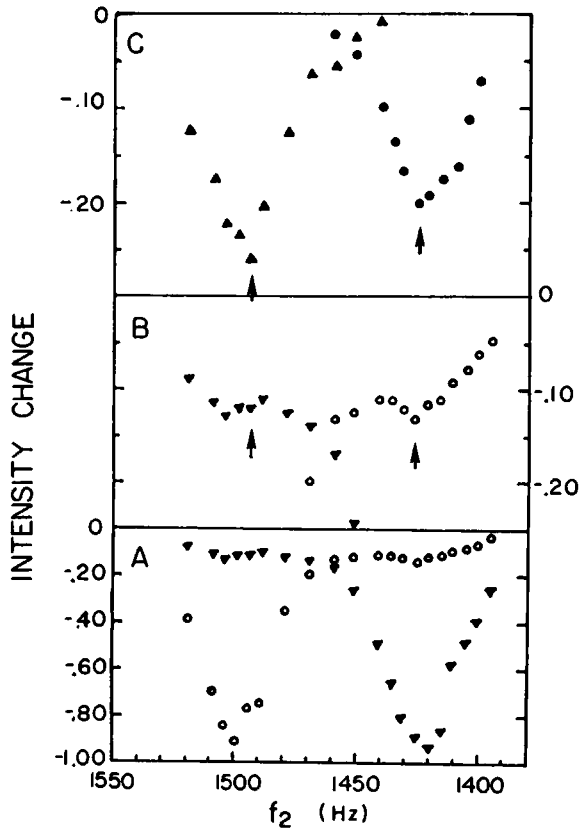

FIGURE 5 (*A*) A graph of decoupler frequency, f_2, vs. intensity change of D-Phe[7]Hα (open circles) and Orn[2]Hα (triangles) protons. Note that when f_2 = 1,497 Hz (the resonant frequency of D-Phe[7]Hα) an intensity change of one proton is detected. When f_2 = 1,420 Hz (the resonant frequency of Orn[2]Hα) the NOE at the frequency of D-Phe[7]Hα is −0.14. The black triangles also show this bimodal effect. (*B*) This is an expanded version of *A*, showing more accurately the intensity changes at Orn[2]Hα and D-Phe[7]Hα upon irradiation of the corresponding multiplet. (*C*) NOEs observed at Asn[8]NH (triangles) and Leu[3]NH (circles) when the decoupler frequency was varied through Hα multiplets of Orn[2] and Phe[7].

one hand and the detection of several proton-proton NOEs for the efficiently relaxed protons (e.g., Orn[2]Hα).

The intraresidue and interresidue NOEs observed in Figs. 2, 3, and 4 and in all NOE experiments, are summarized in Tables I, II, and III. The following types of interactions were observed: (*a*) NOEs in the fragments N*H*(*i*)—*H*α(*i*), ϕNOEs, (*b*) NOEs in the fragment *H*α(*i*)—N*H*(*i* + 1), ψNOEs, (*c*) χ^1NOEs between α and β protons in a given residue, (*d*) NOEs between NH and side chain protons within a residue, (*e*) NOEs between NH (or Hα) of a residue and side chain protons of an adjacent residue, (*f*) NOEs between carboxamide side chain protons and protons of the same or adjacent residues, (*g*) NOEs between backbone amide protons on nonadjacent and adjacent residues, (*h*) NOEs between alpha protons of residues separated in the sequence by more than one residue. NOEs such as *a*–*f* above can be used for sequencing, and NOEs such as *g* and *h* can detect chain folding and transannular interactions.

TABLE I
NOEs BETWEEN BACKBONE ALPHA AND AMIDE PROTONS

Irradiated proton Hα (i)	NH (i)		NH (i + 1)	
	Observed NOE × 10^2	Corrected NOE × 10^2	Observed NOE × 10^2	Corrected NOE × 10^2
Val^1 Hα	−3.1	−3.1	−12.6	−12.6
	(−5.6)*	(−5.6)	(−29.2)	(−25.0)
Orn^2Hα	−2.9	−2.9	−13.0	−12.9
	(−2.4)	(−2.3)	(−15.0)	(−14.8)
Leu^3Hα	−1.7	−1.7	−9.1	−9.1
	(−4.3)	(−3.5)	(−25.0)	(−19.0)
D-Phe^4Hα	−3.5	−3.3		
	(−4.3)	(−4.3)		
Pro^5Hα			−7.0‡	‡
			(−3.4)‡	‡
Phe^6Hα	−12.9‡	‡	−14.2§	−13.9§
	‡	‡	(−32.3)‖	(−31.1)‖
D-Phe^7Hα	−17.0¶	−16.7¶	−17.0¶	−16.7¶
	(−18.2)**	(−18.0)**	(−18.2)**	(−18.0)**
Asn^8Hα	−14.2§	−13.9§	−3.9	−2.8
	(−32.3)‖	(−31.1)‖	(−17.1)	(−7.2)
Gln^9Hα	−2.0	−2.0	−1.1	−1.1
	(−6.5)	(−6.4)	(−3.1)	(−2.9)
Tyr^{10}Hα	−2.2	−1.8	−0.0	−0.0
	(−7.3)	(−6.4)	(−2.8)	(−2.4)

*Parentheses refer to the reverse NOE observed at the various $H\alpha^i$ column 1 when NH^i or NH^{i+1} were irradiated.
‡Due to overlap with the aromatic ring protons correction was not performed and reverse NOEs were difficult to obtain or measure.
§Hα(6) and Hα(8) overlap and both give NOEs at NH(7).
‖Since NH(7) and NH(8) overlap and Hα(6) and Hα(8) also overlap, the observed NOE is the $(\psi_7^+ + \phi_8^-)$ NOE.
¶NH(7) and NH(8) overlap. This NOE is the $(\phi_7^- + \psi_7^+)$ NOE.
**This is the $(\phi_7^+ + \psi_8^-)$ NOE.

Quantitation of NOEs and σ Values

It has been shown for gramicidin S (5, 6) that the intensity changes measured directly from NOEDS have to be corrected for (*a*) decoupler spillover and hence for NOEs arising from the partially saturated protons and, (*b*) cross-relaxation effects. Complications in both detection and quantitation of certain tyrocidine A NOEs arose from overlap of resonances. The latter included: Phe^6NH and aromatic ring protons, Phe^7NH and Asn^8NH, and Phe^6Hα and Asn^8Hα. This meant that NOEs between the following pairs of protons were not directly evaluated: (*a*) the ψNOEs between Phe^6Hα/Phe^7NH, (*b*) the φNOEs between Phe^6NH/Phe^6Hα and Phe^7NH/Phe^7Hα, and (*c*) the ψNOEs between Phe^7Hα/Asn^8NH. Consequently, the NOE ratio method could not yield $r\phi$ and $r\psi$ interproton distances along the Pro^5, Phe^6, D-Phe^7, Asn^8 sequence directly from $\phi^\pm$ and $\psi^\pm$ NOEs. Fortunately, some of these distances were evaluated directly from scalar coupling constants or indirectly from corrected NOE data and the known correlation times (see below). All the corrected NOEs (σ/R) in Tables I, II, and III were obtained by correcting for partial saturation and cross-relaxation.

TABLE II
NOEs BETWEEN BACKBONE AND SIDE CHAIN PROTONS

Irradiated proton	H(*i* − 1)				H(*i*)			
	Observed NOE		Corrected NOE		Observed NOE		Corrected NOE	
	Hβ1	Hβ2	Hβ1	Hβ2	Hβ1	Hβ2	Hβ1	Hβ2
Val[1]Hα					−5.7			
Orn[2]NH					−2.5*			
Hα					−8.6*			
Leu[3]NH					−1.4	−1.4		
Hα					−2.7	−2.5		
D-Phe NH					−6.3	−4.5		
Hα					−15.4§	−1.2		
Pro[5]Hα					−6.5	−7.3		
Phe[6]Hα					−9.1*		−8.5*	
					(−11.0)*			
D-Phe[7]NH	−6.2*				−8.5‡	−6.9		
	(−4.0)*		(−3.0)*		(−3.9)‡	(6.0)	(−2.4)‡	(−6.0)
Hα					−8.4	−2.6	−8.2	−0.8
					(−7.9)	(−3.3)	(−7.4)	(−1.7)
Asn[8]NH	−8.5‡					−8.5‡		
	(−3.9)‡		(−2.4)‡					
Hα					−11.2	−11.4	−8.2	−8.4
					(−21.6)	(−22.8)	(−14.2)	(−18.1)
Gln[9]NH	−14.4	−7.7	−12.8	−2.5	−5.1*			
	(−13.8)	(−5.7)	(−12.5)	(−1.5)				
Hα					−10.2*			
Tyr[10]NH	−2.2*				−7.7*			
Hα					−15.4§			

Parentheses correspond to reverse NOEs observed at NH or Hαs, respectively.
*Hβ1 and Hβ2 are degenerate.
‡NH(7) and NH(8) overlap and Hβ1(7) and Hβ2(8) overlap.
§Hα(4) and Hα(10) overlap and Hβ1(4) and Hβ(10)s overlap.

The cross-relaxation parameters σ_{ij} and σ_{ji} between protons were evaluated from the product of appropriate NOEs with selective excitation proton spin-lattice relaxation rates, R_i and R_j. The latter are shown in Table V. Again owing to spectral overlap, some values are missing. In most cases, for a pair of protons, only σ_{ij} or σ_{ji} was evaluated for reasons of spectral overlap.

rφ and rψ Interproton Distances from NOE Ratios

Jones et al. (9, 10) have calculated $r\phi$ and $r\psi$ distances from ϕ^+, ϕ^-, ψ^+, and ψ^- NOEs using the NOE ratio method (8). The latter assumed that in the peptide fragment N(i)H_A—C(i)H_B—CO—N(i + 1)H_C—C(i + 1)H_D—CO—N(i + 2)H_E—C(i + 2)H_F—CO.

$$\frac{\mathrm{NOE}\,\overrightarrow{\mathrm{AB}}}{\mathrm{NOE}\,\overrightarrow{\mathrm{CB}}} = \frac{r_{\mathrm{CB}}^6}{r_{\mathrm{AB}}^6} \rightarrow \frac{r\psi^-(i)}{r\phi^+(i)} \tag{1}$$

$$\frac{\mathrm{NOE}\,\overrightarrow{\mathrm{BC}}}{\mathrm{NOE}\,\overrightarrow{\mathrm{DC}}} = \frac{r_{\mathrm{DC}}^6}{r_{\mathrm{BC}}^6} \rightarrow \frac{r\phi^-(i+1)}{r\psi^+(i)} \tag{2}$$

$$\frac{\text{NOE }\overrightarrow{\text{CD}}}{\text{NOE }\overrightarrow{\text{ED}}} = \frac{r_{\text{ED}}^6}{r_{\text{CD}}^6} \rightarrow \frac{r\psi^-(i+1)}{r\phi^+(i+1)} \tag{3}$$

$$\frac{\text{NOE }\overrightarrow{\text{DE}}}{\text{NOE }\overrightarrow{\text{FE}}} = \frac{r_{\text{FE}}^6}{r_{\text{DE}}^6} \rightarrow \frac{r\phi^-(i+2)}{r\psi^+(i+1)}. \tag{4}$$

The NOEs in these equations have to be the corrected values in Table I; the interproton distances r_{ij} are designated $r\phi$ or $r\psi$ whether they depend on the dihedral angle ϕ or ψ. Several points can be made: (*a*) since the NOE ratios are measured experimentally one known distance gives the other distance, (*b*) the NOEs involved in the ratio must be measured to the

TABLE III

TRANSANNULAR CHAIN-FOLDING AND MISCELLANEOUS NOEs BETWEEN PROTONS *i* AND *j*. PARENTHESES REFER TO REVERSE NOEs WHERE *j* WAS IRRADIATED AND *i* OBSERVED

H(*i*)	H(*j*)	NOE		Type of NOE
		Observed	Corrected	
Val^1NH	$Tyr^{10}NH$	−6.6	−6.6	a
		(−9.5)	(−9.5)	
Gln^9NH	$Tyr^{10}NH$	−6.2	−4.2	a
		(−4.0)	(−2.0)	
D-$Phe^4H\alpha$	$Pro^5H\delta1$	−12.1	−9.6	b
		(−16.6)	(−13.4)	
D-$Phe^4H\alpha$	$Pro^5H\delta2$	−11.1	−8.3	b
		(−14.8)	(−10.8)	
$Pro^5H\delta1$	$Pro^5H\delta2$	−30.5	−29.4	c
		(−30.6)	(−29.6)	
Asn^8NH	Val^1NH	−2.4	−2.4	d
$Orn^2H\alpha$	D-$Phe^7H\alpha$	−8.8	−6.6	d
		(−9.2)	(−6.9)	
$Orn^2H\alpha$	Asn^8NH	−2.8	−1.7	d
		(−4.8)	(−2.8)	
D-$Phe^7H\alpha$	Leu^3NH	−2.1	−1.2	d
		(−2.8)	(−1.5)	
$Tyr^{10}NH$	$Tyr^{10}H\delta$	−3.2	−2.4	e
$Tyr^{10}NH$	$Tyr^{10}H\epsilon$	−1.1	−0.6	e
$Tyr^{10}H\alpha$	$Tyr^{10}H\delta$	−3.4	−4.4	e
$Tyr^{10}H\alpha$	$Tyr^{10}H\epsilon$	0.0	−2.0	e
$Tyr^{10}H\delta$	$Tyr^{10}H\epsilon$	−20.8	−19.0	c
		(−18.5)	(−16.7)	
$Asn^8H\beta1$	$Asn^8H\beta2$	−37.5	−36.0	c
		(−33.8)	(−32.1)	
$Asn^8H\delta2$	$Asn^8H\delta1$	−30.0	−30.0	c
$Asn^8H\beta2$	$Asn^8H\delta1$	−6.6	−6.6	c
$Asn^8H\beta2$	$Asn^8H\delta2$	−2.0	0.0	c
$Asn^8H\beta1$	$Asn^8H\delta2$	−2.0	0.0	c

a. β-turn.

b. $\psi^+(4)$; type II′ β-turn dihedral angle.

c. Intraresidue side chains.

d. Transannular and antiparallel β-pleated sheet.

e. Intraresidue backbone-side chain.

TABLE IV
INTERPROTON DISTANCES (Å) CALCULATED FROM THE RATIOS OF σ_{ij}/R^{i} VALUES IN TABLES I, II, AND III

	$^3J_{NHCH}$ (Val^1) = 9.5 Hz $^3J_{(1)}$	$^3J_{NHCH}$ (Orn^2) = 9.9 Hz $^3J_{(2)}$	$^3J_{NHCH}$ (Leu^3) = 9.3 Hz $^3J_{(3)}$	$^3J_{NHCH}$ (D-Phe^4) = 4.4 Hz $^3J_{(4)}$	$^3J_{NHCH}$ (Gln^9) = 5.4 Hz $^3J_{(9)}$	$^3J_{NHCH}$ (Tyr^{10}) = 10.5 Hz $^3J_{(10)}$	Avg.	(Pro^{5}Hδ1 – Pro^{5}Hδ2)	Avg.
Val^{1}NH-Val^{1}Hα	*2.9**	3.0	2.9	3.1	2.9	2.9	2.9 ± 0.1	2.9 2.8	2.9
Val^{1}Hα-Orn^{2}NH	2.3	2.3	2.2	2.4	2.3	2.2	2.3 ± 0.1	2.2 2.2	2.2
Orn^{1}NH-Orn^{2}Hα	2.9	*3.0**	2.9	3.0	2.9	2.8	2.9 ± 0.1	2.9 2.8	2.8
Orn^{2}Hα-Leu^{3}NH	2.1	2.2	2.1	2.2	2.1	2.1	2.2 ± 0.1	2.1 2.1	2.1
Leu^{3}NH-Leu^{3}Hα	3.0	3.0	*2.9**	3.1	3.0	2.9	3.0 ± 0.1	3.0 2.9	2.9
Leu^{3}Hα-D-Phe^{4}NH	2.3	2.3	2.2	2.4	2.2	2.2	2.3 ± 0.1	2.2 2.2	2.2
D-Phe^{4}NH-D-Phe^{4}Hα	2.7	2.8	2.7	*2.8**	2.7	2.7	2.7 ± 0.1	2.7 2.6	2.6
D-Phe^{4}Hα-Pro^{5}Hδ1	2.2	2.2	2.1	2.3	2.2	2.1	2.2 ± 0.1	2.1	
D-Phe^{4}Hα-Pro^{5}Hδ2	2.3	2.3	2.2	2.4	2.2	2.2	2.3 ± 0.1	2.2	
Pro^{5}Hδ1-Pro^{5}Hδ2	1.8	1.8	1.8	1.9	1.8	1.8	1.8 ± 0.1	*1.8‡*	
	1.8	1.9	1.8	1.9	1.8	1.8	1.8 ± 0.1		
Orn^{2}Hα-D-Phe^{7}Hα	2.4	2.4	2.4	2.5	2.4	2.4	2.4 ± 0.1	2.4 2.3	2.4
Leu^{3}NH-D-Phe^{7}Hα	3.1	3.1	3.0	3.2	3.1	3.0	3.1 ± 0.1	3.0 3.0	3.0
Orn^{2}Hα-Asn^{8}NH	3.0	3.1	3.0	3.2	3.0	3.0	3.0 ± 0.1	3.0 2.9	3.0
Val^{1}NH-Tyr^{10}NH	2.4	2.5	2.4	2.5	2.4	2.4	2.4 ± 0.1	2.4 2.3	2.4
Asn^{8}NH-Val^{1}NH	3.1	3.1	3.0	3.2	3.0	3.0	3.1 ± 0.1	3.0 2.9	3.0
Val^{1}NH-Tyr^{10}Hα	3.5	3.5	3.4	3.6	3.5	3.4	3.5 ± 0.1	3.4 3.3	3.4
Tyr^{10}NH-Tyr^{10}Hα	3.0	3.1	3.0	3.2	3.0	*3.0**	3.0 ± 0.1	3.0 2.9	2.9
Tyr^{10}NH-Gln^{9}Hα	3.3	3.3	3.2	3.4	3.3	3.2	3.3 ± 0.1	3.2 3.2	3.2
Gln^{9}NH-Tyr^{10}NH	2.6	2.7	2.6	2.7	2.6	2.6	2.8 ± 0.1	2.6 2.5	2.7
	2.9	2.9	2.8	3.0	2.9	2.8		2.8 2.8	
Gln^{9}Hα-Gln^{9}NH	2.9	2.9	2.8	3.0	*2.9**	2.8	2.9 ± 0.1	2.8 2.8	2.8
Gln^{9}NH-Asn^{8}Hα	2.7	2.8	2.7	2.8	2.7	2.7	2.7 ± 0.1	2.7 2.6	2.6
Gln^{9}NH-Asn^{8}Hβ1	2.1	2.2	2.1	2.2	2.1	2.1	2.1 ± 0.1	2.1 2.0	2.1

(continued)

TABLE IV (continued)

	$^3J_{NHCH}$ (Val^1) − 9.5 Hz $^3J_{(1)}$	$^3J_{NHCH}$ (Orn^2) − 9.9 Hz $^3J_{(2)}$	$^3J_{NHCH}$ (Leu^3) − 9.3 Hz $^3J_{(3)}$	$^3J_{NHCH}$ (D-Phe^4) − 4.4 Hz $^3J_{(4)}$	$^3J_{NHCH}$ (Gln^9) − 5.4 Hz $^3J_{(9)}$	$^3J_{NHCH}$ (Tyr^{10}) − 10.5 Hz $^3J_{(10)}$	Avg.	(Pro^{5}Hδ1 − Pro^{5}Hδ2)	Avg.
Gln^{9}NH-Asn^{8}Hβ2	3.1	3.1	3.0	3.2	3.0	3.0	3.1 ± 0.1	3.0 2.8	3.0
Asn^{8}Hα-Asn^{8}Hβ1	2.4	2.4	2.4	2.5	2.4	2.4	2.4 ± 0.1	2.4 2.3	2.3
	2.3	2.4	2.3	2.4	2.3	2.2		2.2 2.3	
Asn^{8}Hα-Asn^{8}Hβ2	2.3	2.4	2.3	2.4	2.3	2.3	2.4 ± 0.1	2.3 2.4	2.4
	2.5	2.6	2.4	2.6	2.5	2.4		2.2 2.4	
Asn^{8}H 1-Asn^{8}Hβ2	1.8	1.8	1.8	1.9	1.8	1.8	1.9 ± 0.1	1.8 1.8	1.8
	1.9	1.9	1.8	2.0	1.9	1.8		1.9 1.9	
	1.9	1.9	1.8	2.0	1.9	1.8		1.8 1.8	
	2.0	2.0	1.9	2.0	2.0	1.9		1.8 1.9	

*Distances calculated directly from ^3J derived ϕ angle and used to calculate the other distances in the column.
‡Distance of geminal protons calculated from standard bond lengths and bond angles (42).

same proton, (*c*) the ϕ distances $r\phi_{AB}(i)$, $r\phi_{CD}(i+1)$ and $r\phi_{EF}(i+1)$ can be derived from scalar coupling constants, $^3J_{NHH\alpha}$, and appropriate Karplus curves (19), (*d*) two $r\phi$ distances can yield each $r\psi$ distance, e.g., $r\phi(i)$ $(\overrightarrow{AB})$ and $r\phi(i+1)$ $(\overrightarrow{DC})$ can yield $r\psi(i)$ $(\overrightarrow{BD})$ and $r\phi(i+1)$ $(\overrightarrow{CD})$, and $r\phi(i+1)$ $(\overrightarrow{FE})$ can yield $r\psi(i+1)$ $(\overrightarrow{DE})$.

As pointed out by Jones et al. (9, 10) by taking ratios of the ratios in equations 1, 2, 3, and 4, any distance, e.g., $r\phi(i)$, can be used to calculate any other $r\phi$ or $r\psi$ distance (i.e., we are not restricted to using NOEs between adjacent pairs of protons).

$r\phi$ and $r\psi$ Distances from Scalar Coupling Constants

The above rationale permitted evaluation of all the distances in Table IV from scalar coupling constants; the same $r\psi$ distances calculated from several $r\phi$ distances are in good agreement. An error analysis of this type of data is published (9).

For the Val^1, Orn^2, Leu^3, Phe^6, D-Phe^7, and Tyr^{10} residues the coupling constants were so large that only two possible ϕ angles and two possible $r\phi$'s (not four) were obtained for each and furthermore, within the accuracy of coupling constant measurements, the two $r\phi$ values were equal for each of these residues. For the D-Phe^4 and Gln^9 residues the four ϕ angles per $^3J_{NHH\alpha}$ value reduced to only two $r\phi$ distances; 2.4 and 2.8 Å for *D*-Phe^4 and 2.3 and 2.9 Å for Gln^9. In both cases only the larger $r\phi$ gave distances consistent with the results based on the other coupling constants. In this way some of the degeneracy in the calculated distances was removed.

TABLE V

SELECTIVE SPIN-LATTICE RELAXATION RATES IN s^{-1}

Residue	NH	Hα	Hβ1	Hγ2	Hδ1	Hε
Orn^2	3.4	4.0				
Leu^3	4.1					
D-Phe^4	3.6					
Pro^5		1.6		3.9	4.8	
D-Phe^7	3.6*	4.0				
Asn^8	3.8*		6.1			
Gln^9	4.6	1.8				
Tyr^{10}	3.4				1.5	1.2

*D-Phe^{7}NH and Asn^{8}NH are overlapped.

rϕ and rψ Distances from Geminal Interproton Distances

The validity of the previous calculations rests upon whether the tyrocidine A ring is rigid or whether the correlation times for ϕ or ψ internal motion cancel or whether the actual measurements are sensitive or insensitive to the actual correlation times for ϕ or ψ motion. These questions will be treated later but confirmation of the distances obtained from NOE ratios and "scalar coupling constant-derived-calibration-distances" came from using a calibration distance that is independent of correlation times for ϕ or ψ motion or conformation; this is the geminal interproton distance for the delta CH_2 group of Pro^5 in tyrocidine A. A similar approach was used for gramicidin S (9, 10).

Both $r\phi$ and $r\psi$ distances were calculated for tyrocidine A based upon the NOE ratios and

TABLE VI

VALUES OF σ_{ij}* CALCULATED FROM $\sigma_{ij}/R^i\ (\tilde{i})$ TERMS AND $R^i(\tilde{i})$

	Orn^{2}NH	Leu^{3}NH	D-Phe^{4}NH	Asn^{8}NH	Gln^{9}NH	Tyr^{10}NH	Pro^{5}Hδ1	D-Phe^{7}Hα	Asn^{8}Hβ1	Tyr^{10}Hε
Val^{1}Hα	−0.43									
Orn^{2}Hα	−0.099	−0.53		−0.065‡				−0.26		
	−0.092	−0.59		−0.072‡				−0.28		
Leu^{3}Hα		−0.70	−0.33							
D-Phe^{4}Hα			−0.12				−0.46			
D-Phe^{7}Hα		−0.59*								
		−0.049*								
Asn^{8}Hα					−0.13				−0.50	
Gln^{9}Hα					−0.092	−0.037				
					−0.12	−0.052				
Tyr^{10}Hα						−0.061				
Pro^{5}Hδ2							−1.4			
Val^{1}NH						−0.22				
Asn^{8}Hβ2					−0.069				−2.0	
Asn^{8}Hβ1					−0.58					
					−0.78					
D-Phe^{7}Hβ1								−0.30		
Gln^{9}NH						−0.092				
Tyr^{10}Hδ										−0.23
										−0.26

*When two σ appear in the table they correspond to $\sigma_{ij} = \mathrm{NOE}(j \rightarrow i) \times R^i$ and $\sigma_{ji} = \mathrm{NOE}(i \rightarrow j) \times R^j$. In general $\sigma_{ij} = \sigma_{ji}$.

‡Asn^{8}NH overlapped with D-Phe^{7}NH.

$r(\text{Pro}^5\text{H}\delta 1\text{-Pro}^5\text{H}\delta 2) = 1.77$ Å. The $r\phi$ distances (Table IV) agreed well with the same distances calculated directly from ${}^3J_{NHH\alpha}$ values (which reflect through bond interaction) proving the validity of the latter approach. The $r\phi$ and $r\psi$ distances agreed with those calculated in the previous section assuming a knowledge of $r\phi$ for each residue. Considerable confidence can therefore be placed upon the calculated distances, the assumptions and the procedures of this and the previous sections.

$r\phi$ and $r\psi$ Distances from the Cross-relaxation Parameters

The cross-relaxation parameters, σ_{ij} and σ_{ji}, should be the same for any pair of protons in tyrocidine A. The σ values were calculated from the corrected NOEs (σ/R) and spin-lattice relaxation rates, $R^i(\bar{i})$ and $R^i(\bar{j})$. In most cases only one value was obtained; these are shown in Table VI. This procedure is entirely analogous to the use of NOEs alone.

The $r\phi$ and $r\psi$ distances calculated from σ ratios are shown in Table VII. Once again r_{geminal} and ${}^3J_{NHH\alpha}$ distances were used as calibration distances. Here therefore, we have an example of $r\phi$ and $r\psi$ distances calculated from a combination of NOEs and proton relaxation rates using two classes of calibration distances. That the various $r\phi$ and $r\psi$ distances agree substantially with those calculated from only NOE measurements in the last section again gives faith in both the measurements and assumptions.

Correlation Times from σ Parameters: $r\phi$ and $r\psi$ Distances from Correlation Times

$$\sigma_{ij} = \left(\frac{\gamma^4 h^2}{2\pi}\right)(r_{ij}^{-6})\left(\frac{3\tau_c^{ij}}{5 + 20\omega_0^2(\tau_c^{ij})^2} - \frac{\tau_c^{ij}}{10}\right),$$

where γ is the magnetogyric ratio of proton, h, Planck's constant, ω_0, the larmor precession frequency.

Using the σ values and five of the ${}^3J_{NHH\alpha}$ derived distances, the correlation time for the backbone of tyrocidine A was found to be 1.33×10^{-9} s. This, as expected, is slightly slower than the value for gramicidin S (15, 16, 17). The σ value between the geminal δ protons of Pro[5] was used to calculate the correlation time, $\tau_c^{\delta 1\delta 2}$, from their interproton distance, 1.77 Å.

TABLE VII

INTERPROTON DISTANCES CALCULATED BY THE σ RATIO METHOD USING THE PROLINE r(gem) AND $r\phi$ DISTANCES AS CALIBRATION. ONLY $r\phi$ DISTANCES FOR RESIDUES 2, 3, 4, 9, AND 10 WERE USED.

	${}^3J_{(2)}$	${}^3J_{(3)}$	${}^3J_{(4)}$	${}^3J_{(9)}$	${}^3J_{(10)}$	Avg.*	Pro[5] $r(\delta 1 - \delta 2)$	Avg.
Val[1]Hα-Orn[2]NH	2.3	2.2	2.3	2.3	2.2	2.2 ± 0.1	2.2	
	2.3			2.2				
Orn[2]NH-Orn[2]Hα	*3.0‡*	2.8	2.9	3.0	2.8	2.9 ± 0.1	2.8	2.8
		2.8	2.9	2.9	2.7		2.8	
Orn[2]Hα-Leu[3]NH	2.2	2.1	2.2	2.2	2.1	2.2 ± 0.1	2.1	2.1
	2.2	2.1	2.1	2.2	2.0		2.0	
	2.2			2.2				
	2.2			2.1				
Orn[2]Hα-D-Phe[7]Hα	2.5	2.4	2.4	2.5	2.3	2.4 ± 0.1	2.3	2.3

(continued)

TABLE VII (continued)

	$^3J_{(2)}$	$^3J_{(3)}$	$^3J_{(4)}$	$^3J_{(9)}$	$^3J_{(10)}$	Avg.*	Pro^5 $r(\delta 1 - \delta 2)$	Avg.
	2.5	2.3	2.4	2.5	2.3		2.3	
	2.5			2.4				
	2.5			2.4				
D-Phe^{7}Hα-Leu^{3}NH	3.2	3.0	3.1	3.2	3.0	3.2 ± 0.1	3.0	3.1
	3.3	3.1	3.2	3.3	3.1		3.1	
	3.2			3.1				
	3.3			3.2				
Leu^{3}NH-Leu^{3}Hα	3.1	*2.9*‡	3.0	3.1	2.9	3.0 ± 0.1	2.9	
	3.1			3.0				
Leu^{3}Hα-D-Phe^{4}NH	2.4	2.3	2.4	2.4	2.2	2.4 ± 0.1	2.3	
	2.4			2.3				
D-Phe^{4}NH-D-Phe^{4}Hα	2.9	2.7	*2.8*‡	2.9	2.7	2.8 ± 0.1	2.7	
	2.9			2.8				
D-Phe^{4}Hα-Pro^{5}Hδ1	2.2	2.1	2.2	2.3	2.1	2.2 ± 0.1	2.1	
	2.3			2.2				
Pro^{5}Hδ1-Pro^{5}Hδ2	1.9	1.8	1.8	1.9	1.8	1.8 ± 0.1	*1.8*§	
	1.9			1.8				
Gln^{9}NH-Gln^{9}Hα	2.8	2.7	2.8	*2.9*‡	2.7	2.8 ± 0.1	2.7	2.7
	2.9	2.8			2.7		2.7	
	2.9							
	3.0							
Tyr^{10}NH-Tyr^{10}Hα	3.2	3.0	3.1	3.2	*3.0*‡	3.1 ± 0.1	3.0	
	3.2			3.1				
Gln^{9}NH-Tyr^{10}NH	2.7	2.8	2.9	3.0	2.8	2.8 ± 0.1	2.8	2.7
	2.8	2.6	2.7	2.8	2.6		2.6	
	2.9			2.8				
	3.0			2.7				
Tyr^{10}NH-Val^{1}NH	2.5	2.4	2.5	2.6	2.4	2.5 ± 0.1	2.4	
	2.6			2.5				
Gln^{9}Hα-Tyr^{10}NH	3.4	3.3	3.4	3.4	3.2	3.4 ± 0.1	3.2	3.3
	3.5	3.3	3.4	3.5	3.4		3.3	
	3.2			3.3				
	3.3			3.4				
Asn^{8}Hα-Gln^{9}NH	2.8	2.6	2.7	2.8	2.6	2.7 ± 0.1	2.6	
	2.8			2.7				
Asn^{8}Hα-Asn^{8}Hβ1	2.3	2.2	2.2	2.3	2.1	2.2 ± 0.1	2.2	
	2.2			2.2				
Asn^{8}Hβ1-Gln^{9}NH	2.2	2.1	2.1	2.2	2.0	2.1 ± 0.1	2.0	2.0
	2.2	2.0	2.1	2.1	2.0		2.0	
	2.1			2.1				
	2.1			2.0				
Asn^{8}Hβ2-Gln^{9}NH	3.1	3.0	3.1	3.2	2.9	3.1 ± 0.1	3.0	
	3.2			3.0				
Asn^{8}Hβ2-Asn^{8}Hβ1	1.8	1.7	1.8	1.8	1.7	1.8 ± 0.1	1.7	
	1.8			1.8				
Tyr^{10}Hδ-Tyr^{10}Hϵ	2.5	2.4	2.5	2.6	2.4	2.5 ± 0.1	2.4	2.4
	2.5	2.4	2.5	2.5	2.3		2.4	
	2.6			2.5				
	2.5			2.4				

*Represents an average of each distance calculated from all ^3J derived from $r\phi$ distances.
‡Distances were calculated from ^3J derived ϕ angle and used to calculate the other distances in the column.
§Distance of geminal protons calculated from standard bond lengths and bond angles (42).

This value, 1.19×10^{-9} s, within experimental error, equalled the above correlation time for the ϕ interproton vectors. This result again gives us confidence in the use of the NOE ratio method and σ ratios from NOE and relaxation rates to calculate $r\phi$ and $r\psi$ distances from either ${}^3J_{NHH\alpha}$ or $r(\text{Pro}^5\text{H}\delta 1\text{-Pro}^5\text{H}\delta 2)$ calibration distances.

Another approach to $r\phi$ and $r\psi$ distance measurement would be to use the correlation time to calculate the σ values from known distances, or to calculate $r\phi$, $r\psi$ from known σ values.

It was not possible to unambiguously evaluate $r\phi$ and $r\psi$ values of the Phe^6, D-Phe^7, and Asn^8 residues because of overlap of their NH and/or Hα multiplets as previously explained. Here we will describe how calculations based upon τ_c values can resolve these ambiguities. (*a*) $r\psi$ for D-Phe^7: the sequence of calculations used to obtain $r\psi(7) = 2.1$ Å is shown:

$$
\begin{array}{ccccc}
{}^3J(7) \xrightarrow[\text{curve}]{\text{Karplus}} r\phi(7) \xrightarrow{\tau_c} \sigma_\phi(7) = 0.08_0 \\
\downarrow R^{H\alpha(7)} = 4.0_0\ \text{s}^{-1} \\
\sigma_\psi(7) \xleftarrow{R^{H\alpha(7)}} \psi^-(7)\text{NOE} = 0.16_0 \xleftarrow[= 0.18_0]{[\phi^+(7) + \psi^-(7)]\text{NOE}} \phi^+(7)\ \text{NOE} \\
\downarrow \tau_c \\
r\psi(7) = 2.1\ \text{Å}.
\end{array}
$$

In this sequence the $r\phi(7)$ distance gave the value of $\sigma_\phi(7)$, the cross-relaxation parameter for the NH-Hα vector of D-Phe^7. Division of $\sigma_\phi(7)$ by the selective relaxation rate of Hα(7) gave the $\phi^+(7)$NOE that should be obtained at Hα(7) if NH(7) was irradiated. (The latter was not resolved experimentally because of overlap of the Phe^{7}NH and Asn^{8}NH resonances.) The sum of the $\phi^+(7)$ and $\psi^-(7)$ NOEs obtained by irradiating at the Asn^{8}NH/Phe^{7}NH position was -0.18_0 at the isolated Phe^{7}Hα multiplet. The difference therefore gave the $\psi^-(7)$NOE which, with the experimental $R^{H\alpha(7)}$ and the τ_c (essentially a reversal of the first procedure), gave $r\psi(7) = 2.1$ Å.

A second approach to calculating $r\psi(7)$ used the selective relaxation rates of D-Phe^{7}NH($=3.6\ \text{s}^{-1}$) and Asn^{8}NH($=3.8\ \text{s}^{-1}$) and the sum of $[\phi^-(7) + \psi^+(7)]$ NOEs. The sequence of this calculation was:

$$
\begin{array}{c}
{}^3J(7) \longrightarrow r\phi(7) \xrightarrow{\tau_c} \sigma_\phi(7) \xrightarrow[= 3.6]{R^{NH(7)}} \phi^-(7)\text{NOE} \\
\downarrow [\phi^-(7) + \psi^+(7)]\text{NOE} = -0.16_7 \\
\psi^+(7)\text{NOE} = -0.14_5 \\
\downarrow R^{NH(8)} = 3.8 \\
r\psi(7) = 2.2\ \text{Å} \xleftarrow{\tau_c} \sigma_\psi(7).
\end{array}
$$

In this calculation the values of the selective relaxation rates of the amide protons of D-Phe^7 ($3.6\ \text{s}^{-1}$) and Asn^8 ($3.8\ \text{s}^{-1}$) were used, in spite of the fact that the values could have been inaccurate because their amide protons resonances overlapped. Extension of the above reasoning showed that the experimental values were sufficiently accurate. Since the calculation of $r\psi(7)$ from Asn^{8}NH and D-Phe^{7}NH rates agreed with the results using the relaxation rate of Hα(7) the assumption, procedures, rates etc. are quite reasonable. (*b*) $r\psi$ for D-Phe^6:

$$\begin{array}{c}
{}^3J(8) \longrightarrow r\phi(8) \xrightarrow{\tau_c} \sigma_\phi(8) \xrightarrow{R^{\mathrm{NH(8)}}} \phi^-(8)\mathrm{NOE} \\
{}[\phi^-(8) + \psi^+(6)]\mathrm{NOEs} \\
r\psi(6) \xleftarrow{\tau_c} \sigma_\psi(6) \xleftarrow{R^{\mathrm{NH(8)}}} \psi^+(6)\mathrm{NOE.}
\end{array}$$

In this case, only the NOE sum $[\phi^-(8) + \psi^+(6)] = -0.13_9$ and not the individual NOEs was observed at their overlapping amide resonances due to simultaneous saturation of the overlapping Hα(6) and/or Hα(8). This calculation gave $r\psi(6) = 2.3$ or 2.7 Å due to the fact that $r\phi(8)$ has two possibilities, 2.9 or 2.3 Å.

rφ, rψ Distances and Side Chain Stereochemistry from Backbone-side Chain NOEs and σ Parameters

Extensive spectral overlap in the side chain region of the ^{1}H-NMR spectrum of tyrocidine A prevented a total study of backbone $\rightleftharpoons$ side chain NOEs and σ parameters, but a significant amount of confirmatory and complementary information on ($r\phi$, $r\psi$) distances and side chain stereochemistry was obtained. This included: (*a*) determination of ψ and χ^1 for Asn^8, (*b*) determination of $r\chi$ for D-Phe^7, (*c*) ϕ and χ^1 determination of D-Phe^4 and Gln^9, (*d*) ψ determination of Phe^6, (*e*) carboxamide assignment for Asn^8 and Gln^9, and (*f*) χ^2 determination for Asn^8.

The NH $\rightleftharpoons$ side chain, Hα $\rightleftharpoons$ side chain and side chain $\rightleftharpoons$ side chain NOEs detected for tyrocidine A are shown in Figs. 2, 3, 4, and 6, and the value of the corrected NOEs and σ parameters shown in Tables II and III. To convert this information into $r\phi$, $r\psi$, and $r\chi$ interproton distances NOE ratios or σ ratios with known interproton distances were utilized as described above and the correlation time $\tau_c = 1.33 \times 10^{-9}$ for the tyrocidine A molecule.

This procedure was partly justified by determination of the correlation times from σ parameters (Table VI and known distances) for the Hβ1-HB2, Hδ1-Hδ2, Hδ-Hϵ vectors of Asn^8, Pro^5, and Tyr^{10}. These values, 1.41×10^{-9} s, 1.19×10^{-9} s, 1.30×10^{-9} s, were essentially the same as those for backbone NH-Hα vectors. That certain interproton distances agreed with $r\phi$ and $r\chi$ distances calculated directly from $^3J_{\mathrm{NHH}\alpha}$ or $^3J_{\alpha\beta}$ values and Karplus curves provided additional justification.

Asn⁸ rφ, rψ, and rχ¹ Distances

Both Hβ1 and Hβ2 were shown (5) by scalar coupling constant analysis to be 2.5 Å distant from Hα($^3J_{\alpha\beta1} = 2.6$ Hz and $^3J_{\alpha\beta2} = 4.0$ Hz); the Asn^8 side chain thus spends >85% of its time in the $\chi^1 = +60°$ rotamer. Using the $r\phi(9)$ distances from $^3J_{\mathrm{NHH}\alpha}(9)$, two distances were calculated: (*a*) Hα(8)—NH(9), and (*b*) Hβ1(8)—NH(9). The former, $r\psi(8)$, was used to calculate the $r(\alpha\text{-}\beta1)$, $r(\alpha\text{-}\beta2)$, and $r(\beta1\text{-}\beta2)$ distances while the latter yielded the $r(\alpha\text{-}\beta1)$ and $r(\beta1\text{-}\beta2)$ distances for Asn^8. These data are shown in Tables IV and VII along with similar values for Asn^8 calculated from the $r\phi$ distances of residues Val^1, Orn^2, Leu^3, D-Phe^4, and Tyr^{10}. The $r(\alpha\text{-}\beta1)$, $r(\alpha\text{-}\beta2)$, and $r(\beta1\text{-}\beta2)$ distances, calculated from the r_{geminal} distance of

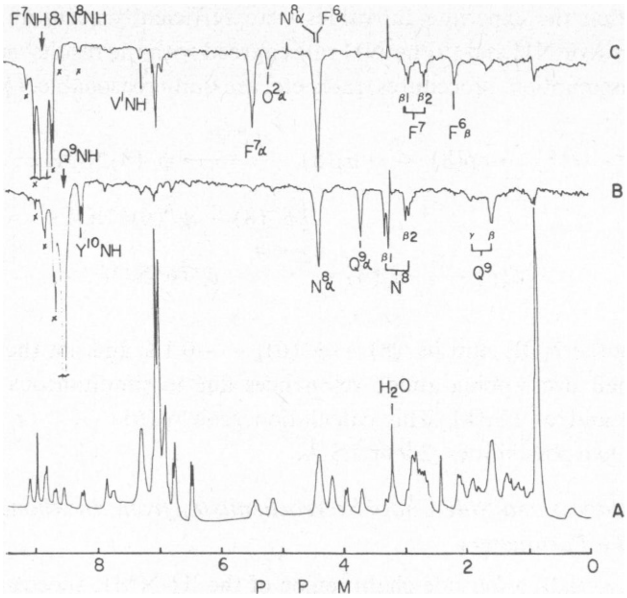

FIGURE 6 (A) The complete ^{1}H-NMR spectrum of tyrocidine A in DMSO-d_6 temperature, 26°C; concentration, 15 mg/ml. (B) NOEDS with f_2 centered at Gln^{9}NH. NOEs are seen at Asn^{8}Hα, Gln^{9}Hα, Asn^{8}Hβ1, Ans^{8}Hβ2, and Gln^{9}Hβ. (C) NOEDS with f_2 centered at the overlapping Phe^{7}NH and Asn^{8}NH resonances. NOEs are seen at Val^{1}NH, Phe^{7}Hα, Orn^{2}Hα, Asn^{8}Hα, Phe^{6}Hα, D-Phe^{7}Hβ1, Phe^{7}Hβ2, and Phe^{6}Hβ. The percentage of the CH_3 and aromatic signals in B and C attributable to NOEs vs. incomplete spectral cancellation of intense peaks is uncertain. Partial saturations of multiplets close to the f_2 frequencies are marked with an x.

Pro^5, are also in these Tables. The agreement between these χ^1 distances and those from rotamer analysis is satisfactory, and the $r(\beta 1\text{-}\beta 2)$ distance, 1.89 ± 0.06 Å, corresponds closely to a typical r_{geminal} distance.

Thus the same χ^1 interproton distances were obtained (*a*) directly from scalar coupling constants, (*b*) by NOE ratio methods, (*c*) by combination of NOEs and relaxation rates. This approach to the study of side chain conformation is therefore satisfactory. Because the interproton distances between Gln^{9}NH, Asn^{8}Hβ1, and Asn^{8}Hβ2 were all evaluated (Tables IV and VII), this defined the ψ angle of Asn^8 as $-170° \pm 10°$. Having uniquely defined $(\psi, \chi^1) = (-170°, +60°)$, information from energy minimization calculations (22) can help resolve which of the four $\phi(8)$ angles are present in tyrocidine A; for *N*-acetyl-asparagine-*N'*-methylamide only $\phi = -154°$ or $-86°$ are allowed and not $\phi = +42°$ or $+79°$. Both $-154°$ and $-86°$ give $r\phi(8) = 2.9$ Å.

$r\chi^1$ Distances of D-Phe^7

A similar calculation for D-Phe^7 from the $(\beta 1 \rightarrow \alpha)$NOE (Table II) gave $r(\alpha\text{-}\beta 1) = 2.4$ Å, $r(\alpha\text{-}\beta 2) = 3.1$ Å, which corresponded well with the gauche conformation indicated by $^3J_{\alpha\beta 1} = 3.5$ Hz and $^3J_{\alpha\beta 2} = 12.0$ Hz. The $r\chi^1$ distances for other side chains were difficult to evaluate from NOE data due to either spectral overlap with other residues, degeneracy of the two β protons or the lack of selective relaxation rate data.

Complementary $r\phi$, $r\psi$, and $r\chi^1$ Information for Other Residues

Although the quantitation of $r\phi$ and $r\psi$ interproton distances other than the above was not achieved, the magnitude of certain observed NOEs qualitatively resolved the equivocal conformations derived only from backbone NOE data or other NMR parameters, e.g., the D-Phe^4 side chain was determined as ~68% in the $\chi^1 = +60°$ rotamer, from its $^3J_{\alpha\beta}$ values and the anomalous upfield shift of the Pro^{5}Hδ2 chemical shift by the D-Phe^4 aromatic ring (17, 23). Despite the difficulty of resolving the Tyr^{10}(Hα→Hβ) and the D-Phe^4(Hα→Hβ) NOEs, the latter were accurate enough to support these conclusions. The (NH→Hβ1) and (NH→Hβ2) NOEs gave additional confirmation of the $\chi^1(4)$ rotamers, but also indicated the ϕ angle should be $+66°$ not $+174°$. Because the Phe^{6}NH was buried under the phenylalanine ring proton peaks, measurement of NOEs related to this amide proton was difficult. The almost degenerate Phe^{6}Hβ's could not provide complementary information to yield its χ^1 conformation which had been determined from $^3J_{\alpha\beta}$ values and the anomalous Pro^{5}Hγ2 chemical shift (17). However, for a fixed $\chi^1(6) = -60°$ and each of the four possible ψ angles derived from two $r\psi(6)$ distances, four pairs of r[NH(7)-Hβ1(6)] and r[NH(7)-Hβ2(6)] distances were calculated. The four pairs of (NH-Hβ1, NH-Hβ2) distances corresponding to one $\chi^1(6) = -60°$ and the ψ angles (148°, 92°, 168°, −48°) were calculated to be A(2.9, 3.9), B(4.1, 4.5), C(2.5, 3.5), and D(3.6, 2.6); only the combinations A, C, and D can account for the observed (NH-Hβ)NOE. As shown above, $r\psi = 2.3$ Å and hence C and D are eliminated leaving only A. Thus the conformation of Phe^6 is $(\phi, \psi, \chi^1) = (-148°, +148°, -60°)$ or $(-92°, +148°, -60°)$.

Many backbone ⇌ side chain NOEs were detected which in principle should have given $\phi(7)$, $\psi(7)$, and $\phi(8)$; however, either the spectral overlap interferred with NOE conversion to distances or the calculated distance was unable to resolve the equivocal angles. The degeneracy of the Gln^{9}Hβ's prevented a complete analysis of its C$^\alpha$H-C$^\beta$H$_2$ spin system by straightforward means. The sum $(^3J_{\alpha\beta1} + {^3J_{\alpha\beta2}}) = 12.5$ Hz was, however, consistent with averaging at the χ^1 level. With this assumption and the NOEs for the NH(9)—Hβ vector (Tables IV and VII) the two ϕ angles $\gamma(9) = -73°$ or $-167°$ from the appropriate Karplus curve were distinguished. The weighted average, $\langle r(\mathrm{NH}-\mathrm{H}\beta)\rangle$, was calculated as 2.59 and 3.24 Å corresponding to $\phi = -73°$ or $-167°$. The latter distance corresponded to a very small NOE whereas the former easily explains the 5% NOE observed at the Hβs when Gln^{9}NH was saturated.

Carboxamide Assignments of Asn^8 and Gln^9 and χ^2 for Asn^8

In the past, assigning a pair of carboxamide resonances to either Gln or Asn residues in a complex peptide has been based only on comparison with model peptide spectra (24, 25). Two types of NOE experiment gave unequivocal carboxamide assignments of the Asn^8 and Gln^9 carboxamides in tryocidine A. The pairing was deduced from NOEs (Table III and Fig. 3) between the four carboxamide signals and the assignment of the Asn^8 pair of carboxamide resonances was achieved by NOEs between them and the Asn^8 beta protons (Table III). The differential NOEs at Asn^8 carboxamide protons (Hδ's) obtained by saturation of the Asn^8 beta protons yielded even more information. After correction for cross-relaxation only the (Hβ1→Hδ1) NOE was significant. This gave $\chi^2 = +90°$ for Asn^8.

Miscellaneous NOEs and Interproton Distances

The NOEs for the $Tyr^{10}H\delta$ and $Tyr^{10}H\epsilon$ were used with their relaxation rates to calculate their $\sigma_{\delta\epsilon}$ and $\sigma_{\epsilon\delta}$ values (Table VI). The σ ratio method and $\sigma_{\epsilon\delta}$ gave $r(H\delta\text{-}H\epsilon) = 2.5$ Å, Table VII; in agreement with 2.4 Å, the value calculated from standard bond lengths and angles.

In this section NOEs and cross-relaxation parameters between NH or Hα backbone protons and the side chains of their own or adjacent residues were used to calculate $r\phi$, $r\psi$, $r\chi^1$, $r\chi^2$ distances, and to assign carboxamide protons to specific residues.

Chain Folding and Transannular NOEs, σ Parameters, and Interproton Distances

The previous sections have described the detection of (*a*) $\phi^{\pm}$, $\psi^{\pm}$, and $\chi^{\pm}$ NOEs, (*b*) NOEs between NH(8), and side chain protons of residues i and $i - 1$, (*c*) miscellaneous NOEs such as those between carboxamide protons of one side chain and protons of the same or neighboring residues. In spite of this large variety and number of NOEs and (cross-relaxation parameters, σ) with which to determine $r\phi$ and $r\psi$ distances, the latter are theoretically consistent with four (ϕ, ψ) combinations per amino acid or 4^{10} secondary conformations per decapeptide.

Many regular folded conformations, such as β-turns, β-pleated sheets, and helices are characterized not only by $r\phi$ and $r\psi$ distances but also by interchain proton-proton distances; each of the latter has a corresponding NOE and σ.

The center six residues of the two chains of tyrocidine A are shown:

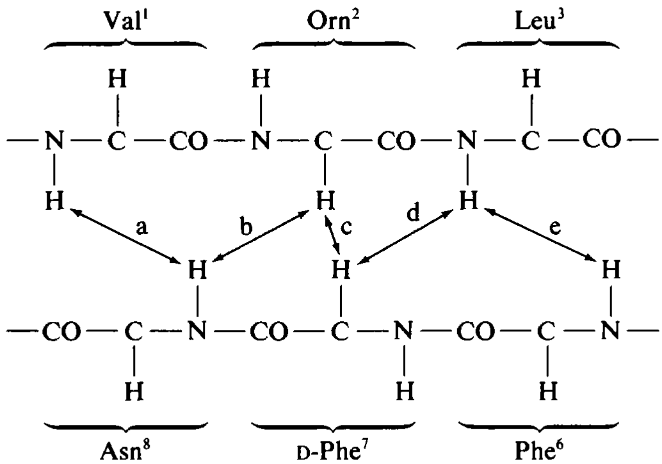

If, as proposed (18, 26), these residues have an approximate antiparallel β-pleated sheet conformation, there should be five detectable intrachain NOEs—designated *a*, *b*, *c*, *d* and *e*. As seen in Fig. 5 and Table III, these NOEs were detected as predicted.

It has already been demonstrated that the series of NOEs $\phi^{\pm}(1) \rightleftharpoons \psi^{\pm}(1) \rightleftharpoons \phi^{\pm}(2) \rightleftharpoons \psi^{\pm}(2) \rightleftharpoons \phi^{\pm}(3)$ . . . etc., can be used to (*a*) sequence peptides (4, 12) and (*b*) quantitatively define all possible secondary conformations (9, 10).

As seen in the diagram the following series of NOEs $Val^1NH \rightleftharpoons Asn^8NH \rightleftharpoons Orn^2H\alpha \rightleftharpoons$ D-$Phe^7H\alpha \rightleftharpoons Leu^3NH \rightleftharpoons Phe^6NH$ qualitatively proved the antiparallel β-pleated sheet nature of this 6-residue moiety of tyrocidine A and are generally diagnostic for the antiparallel vs. parallel β-pleated sheet conformations.

To convert these NOEs and σs in Tables III and VI into interproton distances three methods were used (*a*) σs and correlation times, (*b*) NOE ratio method, and (*c*) σ ratio. The correlation time used was 1.33×10^{-9} s; the Hα(2)-Hα(7) distance was obtained from two distances derived from $^3J(2)$ and $^3J(3)$ with NOEs or σs. Similar techniques gave the NH(1)-NH(8), NH(8)-Hα(2), and Hα(7)-NH(3) distances in Tables IV and VII.

NOEs were measured between the amide protons of the contiguous residues, Gln^{9}NH $\rightleftharpoons$ Tyr^{10}NH and Tyr^{10}NH $\rightleftharpoons$ Val^{1}NH (Figs. 3 *B* and *C*, 6 *B*, and Table III). These NOEs were converted into interproton distances: r[NH(9)-NH(10)] = 2.7 Å and r[NH(10)-NH(1)] = 2.4 Å. Previously (9), it has been shown that in the fragment NH(i)—CαH(i)—CO—NH($i+1$) evaluation of $r\phi(i)$ and $r\psi(i)$ distances gave four possible conformations of residue i. By evaluating r[NH(i)—NH($i+1$)], we have eliminated some of the four conformations. For example, the (ϕ, ψ) angles of Gln^9 were reduced to the ($-73°$, 0) combination by the chain folding distance r[NH(i)—NH($i+1$)] = 2.8 Å. Furthermore, since the error in the NOE measurement increases when the interproton distance exceeds 3 Å, this chain folding distance provides a more accurate measurement of the (ϕ, ψ) angles. In this case Gln^9 was $-10° \pm 15°$). Similarly, within experimental error, the Tyr^{10} residue can have the (ϕ, ψ) combination ($-105° \pm 15°$, $-25° \pm 20°$) but two other combinations, ($-105° \pm 15°$, $-95° \pm 30°$) and ($-135° \pm 15°$, $-95° \pm 30°$) can not be eliminated due to the inaccuracy of $r\psi$ measurement.

Errors and Approximations

In this publication experimental measurements of scalar-J values, NOEs and relaxation rates are reported; the precision of these measurements will be discussed in a manner analogous to a previous publication (9). The effect of a 10% error in an NOE or relaxation rate on correlation times and interproton distances will be traced and it will be demonstrated that in 90% of cases it is <0.2Å.

Certain assumptions concerning relaxation mechanisms and the use of the NOE-ratio method, the σ-ratio method, and σ-values are involved in the calculations. These will be clearly stated and justified in terms of the present and previous publications (1, 2, 8, 9, 21, 27–32).

The Bruker WH270 MHz spectrometer can subtract two spectra to an accuracy of 0.5–2% depending upon the signal to noise ratio of individual spectra; for our NOE measurements spectra (4,000 scans) were subtracted to an accuracy of 0.5–1% and our NOEs were measured three times. To obtain NOEs in the form σ/R in Table I, the intensities measured from spectra (NOE′) were corrected by the equation: NOE = (σ/R) = (NOE′)-(decoupler spillover)-(cross-relaxation). The latter contribution was available (9) since all NOEs to a given proton and all relevant selective relaxation rates were measured. In any event this term never amounted to >10%, in agreement with theory for this size of molecule in DMSO, and therefore had a negligible effect on distances which bear an inverse 6th power relationship to the NOE.

The initial rate approximation (2) was used to obtain relaxation rates from experimental data. The error in this process has been previously discussed (33) and it was shown that for selective relaxation rates of ~4 s^{-1} the error is <10%; for biselective and nonselective relaxation rates larger errors are involved necessitating curve fitting by several exponentials (and types of experiment) to obtain precise (<10% error) relaxation rates; only monoselective rates are used here.

A third experimental variable is involved in this data treatment, namely, the use of experimental J-values to yield $r\phi$ interproton distances (and ϕ angles) from Karplus curves. The error in J-values and the Karplus curves is certainly not >10%.

The general equation used in our error analysis is:

$$\lambda(F) = \left[\left(\frac{\delta F}{\delta \chi_1}\right)^2 \cdot \lambda^2(\chi_1) + \left(\frac{\delta F}{\delta \chi_2}\right)^2 \cdot \lambda^2(\chi_2) + \cdots\right]^{1/2}.$$

NOE ratios were obtained as described above and distances, r_1 and r_2, are governed by the equations:

$$\frac{r_1}{r_2} = \left[\frac{(\sigma/R)_2}{(\sigma/R)_1}\right]^{1/6}$$

and

$$\frac{r_1}{r_2} = \left\{\frac{[(1/T_1^{SE} \cdot (\sigma/R)]_2}{[(1/T_1^{SE} \cdot (\sigma/R)]_1}\right\}^{1/6}.$$

Therefore,

$$r_1 = r_2 \cdot (\sigma/R)_2^{-1/2} \cdot (\sigma/R)_1^{-1/2},$$

and

$$\lambda(r_1) = \left\{(r_2^{-1} \cdot r_1)^2 \cdot \lambda^2(r_2) + \left[\frac{1}{6}\left(\frac{\sigma}{R}\right)_2^{-1} \cdot r_1\right]^2 \cdot \lambda^2\left(\frac{\sigma}{R}\right)_2 + \left[-\frac{1}{6}\left(\frac{\sigma}{R}\right)_1^{-1} \cdot r_1\right]^2 \cdot \lambda^2\left(\frac{\sigma}{R}\right)_1\right\}^{1/2}.$$

The applicability of this equation will be demonstrated for the determination of $r\psi(1)$; using $r_2 = r\phi(2) = 3.0$ Å, and NOEs $(\sigma/R)_1 = 0.25$, and $(\sigma/R)_2 = 0.023$ gives a value of $r_1 = 2.3 \pm 0.2$ Å. Thus a 10% error in every NOE will result in a 2% error in distance from each NOE ratio, e.g., using the NOE-ratio method and $r\phi(2) = 3.0$ Å as "calibration distance" (Table IV), the $r\psi(1)$ is 2.2 ~ 2.4 Å; the $r\psi(2)$ is 2.1 ~ 2.2 Å; and after four NOE-ratios the r(D-Phe^{4}H$^\alpha$—Pro^{5}H$^\delta$) is 1.8 ~ 2.6 Å.

Obtaining distances from σ-ratios (9) instead of NOE-ratios introduces one more variable, the value of T_1^{SE} (the monoselective relaxation time). The agreement between the calculated data in Tables IV and VII by both these methods indicates our T_1^{SE} values are reasonable.

A knowledge of τ_c, the correlation times, permitted a third type of distance measurement directly from σ-values using equations of the form: σ = (constant) · $(1/r^6)$ · (motional factor). We have shown that for the τ_c range used in this publication an error of 20% in τ_c gave a ±0.08 Å error in $r\psi(7)$. When τ_c is obtained from "calibration distances" such as $r\phi(7)$, an error of 0.2 Å in the latter has almost no effect on $r\psi(7)$. Small variations in σ-values, when measured by NOEs and relaxation rates, do not significantly affect distances. Thus using 1.6×10^{-9} s instead of 1.3×10^{-9} s gave $r\psi(7) = 2.2 \pm 0.1$ Å.

To summarize therefore, both the experiments and the data analysis lead to interproton distances in tyrocidine A having a maximum error of 0.2 Å as previously proposed; this estimate is conservative.

Assumptions Involved in Data Analysis

A great deal has now been published to substantiate the use of the NOE-ratio method (1, 9, 10) the σ-ratio method (9), cross-relaxation rates, (9, 27, 28), and relaxation rates to measure distances and correlation times in natural products and biopolymers. It is also becoming clear what limitations and assumptions reside in these methods. These will now be discussed.

One assumption behind the above data treatment is that the mechanism of proton relaxation by other protons and by ^{14}N-nuclei is dipole-dipole. It is assumed that spin-diffusion, chemical shift anisotropy, spin-rotation, cross-correlation, and quadrupole mechanisms do not significantly affect the results. Because we have calculated and evaluated all cross-relaxation rates, it is clear that their magnitude is such that spin-diffusion will not occur. This is borne out experimentally by the lack of detectable (<1%) NOEs at protons distant in the peptide from the protons being saturated. Furthermore, spin-diffusion should not be significant for molecules of molecular weight <2,000 under the conditions of field, temperature, and viscosity used here.

Cross-correlation has not been treated theoretically or detected experimentally in biopolymers. Vold and Vold (29, 30) and others (34) have shown that it should be effective only in rigid, closely coupled systems and can be estimated if the relaxation rates of the individual lines in a spin system are measured. In view of the fact that ignoring this effect in several molecules (9, 28, 31, 35) gave satisfactory agreement between crystal and solution distance, we feel that at least to first-order, cross-correlation can be ignored here. However, more extensive detailed experiments and data treatment are needed to be 100% rigorous in this assumption.

This publication does not deal with internal methyl group rotation and spin-rotation will not effect relaxation of the NH, H^{α}, and H^{β} protons of tyrocidine A. Chemical shift anisotropy will be negligible for protons at 270 MHz.

Considerable evidence exists to justify the dipole-dipole approximation. Many workers have clearly shown it is valid for small organic molecules (1, 3, 28, 29, 30, 35) and it was demonstrated to be operational in ferrochrome (31) whose crystal structure was known. Where it was possible to compare, the $r\phi$, $r\psi$, and transannular distances in gramicidin S agreed with crystal distances (36); Bleich et al. (32) have similar conclusions. Sikakana (personal communication) has compared the interproton distances in cyclo (Pro-Gly-Phe)$_2$ measured by crystallography and by proton relaxation spectroscopy in DMSO; the agreement is better than ±0.2 Å. Thus NH, H^{α}, and H^{β} protons relax predominantly by dipolar mechanisms. The effect of the ^{14}N-nucleus has been discussed by two groups (31, 32) and shown to affect only the amide proton and that by dipolar mechanisms. All of the above discussion is entirely in agreement with the summary of such mechanisms in simple amides given in Noggle and Schirmer (1).

Even when proton relaxation in biopolymers is established to be dipolar, data interpretation is still not necessarily straight forward; other assumptions exist. The NOE- and σ-ratio methods are applicable under two conditions: (*a*) the peptide backbone is rigid and all proton relaxation is controlled by the correlation time for overall motion and (*b*) internal motions at the ϕ, χ, or ω levels (or other) exist but the correlation times affecting NH and H^{α} protons are similar enough that they cancel from the numerator and denominator of the equations for the NOE- and σ-ratio methods. To rigorously justify these assumptions it will be necessary to perform detailed ^{13}C, ^{1}H, and ^{2}H relaxation studies as a function of temperature, frequency, and even solvent. Data already published does however, support the contentions that one of these assumptions is valid. $^{13}C\,T_1$s have been interpreted (37, 38) in terms of a rigid backbone (no ϕ or ψ motion). Thus, at this stage of development of proton relaxation spectroscopy (and NOEs) in the biopolymer area, the approximations in theory and the methods of data analysis are more than adequate to give reasonable interproton distances and correlation times for molecules such as gramicidin S, tyrocidine A, ferrochromes, etc. Extension of this approach to quantitation in proteins is readily envisaged provided spin-diffusion is taken into account. Application to peptides in which individual residue ϕ and ψ motions are different remains a fascinating problem for the future. It also remains to test the existence of peptide motions whose frequencies will not affect T_1 values, and which are not reflected in chemical shifts or exchange broadening.

DISCUSSION

Delineation of (ϕ, ψ) Space From ($r\phi$, $r\psi$) Distances: Methods of Reducing the Number of Possible Secondary Conformations

Each $r\phi$ and $r\psi$ distance determined from proton relaxation parameters corresponds to two ϕ and two ψ dihedral angles. This determination decreases the ϕ value range by two from that found from scalar coupling constants. A decapeptide therefore has 4^{10} possible secondary conformations based upon combined relaxation (through-space coupling) and scalar (through-bond) coupling. This large number seems impossible but this alone represents an advance for it severely limits, and accurately describes, the ϕ, ψ conformational space of the peptide. It should be emphasized that *a priori* energy minimization calculations produce a much larger number of possible conformations. Fortunately, NMR techniques produce a large number of molecular parameters which can be used to exclude a large number of possible (ϕ, ψ) combinations. These include (*a*) heteronuclear coupling constants (39), (*b*) hydrogen bonding of specific amide protons (40, 41), (*c*) proton-chromophore distances (12), (*d*) experimentally derived side chain conformations which exclude certain secondary conformations (12), (*e*) transannular and interchain/folding distances from NOE and relaxation experiments. Ring closure of the peptide if cyclic, energy minimization calculations, CD, Raman, infrared, fluorescence, or spin label studies can also be useful.

Several of these approaches will be used to delineate the conformational moieties present in tryocidine A.

Table VIII shows all $r\phi$ and $r\psi$ distances determined from NOE and proton cross-relaxation parameters. Because some residues were shown to have a unique ϕ or ψ angle only 2^{10} conformations are possible. It has already been proposed that tyrocidine A possesses the type I β-turn/type II′ β-turn/approximately antiparallel β-pleated sheet conformation shown in Fig. 1; one set of the ϕ, ψ angles in Table VIII corresponds closely to this conformation—but it does not prove it. These angles, however, combined with delineation of Val^1NH, Leu[3]NH, Phe[6]NH and Asn[8]NH hydrogen bonds strongly imply such a secondary conformation.

Reduction in the Number of Secondary Conformations of Tyrocidine A Using Non-$r\phi$, $r\psi$ Distances

The postulated β-pleated moiety in this molecule includes six residues: Val[1], Orn[2], Leu[3], Phe[6], D-Phe[7], and Asn[8]. The ϕ angles determined from coupling constants, hydrogen bonds for the Val[1]NH, Leu[3]NH, Phe[6]NH, and solvent exposure of Orn[2]NH and D-Phe[7]NH served as a basis for postulating this secondary conformation for these sequences (23). Here we reported both the possible (ϕ and ψ) angles for these residues based on the interproton distances derived from the relaxation studies. The (ϕ, ψ) angles for each residue derived from $r\phi$ and $r\psi$ distances are summarized in Table VIII. After considering all ^{1}H-^{1}H NOEs the number of possible (ϕ, ψ) combinations was cut down to 2^{10}. One (ϕ, ψ) set: (−144°, +153°), (−138°,

TABLE VIII
ϕ AND ψ TORSIONAL ANGLES FOR TYROCIDINE A

	Torsion angle (A)		Torsion angle (B)	
	ϕ	ψ	ϕ	ψ
Val[1]	−144°	+153°	−144°	+153°
	−96°	+87°	−96°	+87°
Orn[2]	−138°	+128°	−138°	+128°
	−102°	+112°	−102°	+112°
Leu[3]	−144°	+153°	−144°	+153°
	−96°	+87°	−96°	+87°
D-Phe[4]	+66°	−130°	+66°	−130°
	+174°			
	−105°			
	−15°			
Pro[5]	−60° ~ −70°	0° ± 40°	−60° ~ −70°	0° ± 40°
Phe[6]	−148°	+148°	−148°	+148°
	−92°	+92°	−92°	
		+168°		
		−48°		
D-Phe[7]	+132°	−120°	+132°	−120°
	+108°		+108°	
Asn[8]	−154°	+170°	−154°	+170°
	−86°	+50°	−86°	
	+42°			
	+79°			
Gln[9]	−167°	−1°	−73°	−1°
	−73°	−119°		
	+21°			
	+99°			
Tyr[10]	−105°	−25°	−105°	−25°
	−135°	−95°		−95°
			−135°	−95°

Column A contains all possible ϕ, ψ angles consistent with $r\phi$ and $r\psi$ interproton distances and scalar coupling constants; column B contains only those ϕ and ψ angles consistent with all interproton distances measured from transannular, chain folding, and backbone-side chain proton relaxation parameters.

+128°), (−144°, +153°) (−148°, +148°), (+132°, −120°), and (−154°, +170°) for these residues supports the hypothesis of an approximately antiparallel β-pleated conformation, (−139°, +135°), but secondary conformations based upon other combinations of the (ϕ,ψ) angles in Table VIII could not be excluded without the information described below.

Confirmation of the antiparallel β-pleated sheet conformations and of the hydrogen bonds for Val^1, Leu^3, and Asn^8 amide protons came from determination of $r[H\alpha(2)\text{-}H\alpha(7)] = 2.4$ Å, $r(NH(1)\text{-}NH(8)] = 3.1$ Å, $r[H\alpha(2)\text{-}NH(8)] = 3.0$ Å and $r[NH(3)\text{-}H\alpha(7)] = 3.1$ Å. The transannular NOE between [NH(3), NH(6)] could not be observed due to the nature of spectral overlaps, other NMR evidence, e.g. $\Delta\delta/\Delta T$ and k_{HDX}(26) were quite consistent with Phe^6NH being hydrogen bonded. The conclusion that only the antiparallel (ϕ, ψ) angles are consistent with these transannular and $r\phi$, $r\psi$ distances cannot be 100% rigorous until further data are available but model building certainly supports it.

Support for the β-pleated conformation for these six residues came from (a) determination of χ^1 conformations from scalar coupling constants (17) and NOEs and (b) proton-chromophore distance measurements. Residues 6, 7, and 8 had one predominant rotamer: in the predominant $\chi^1 = -60°$, $\chi^2 = 180°$ rotamer the ring current effects of the D-Phe^7 side chain chromophore could account for the downfield shifts of $Orn^2H\alpha$, D-$Phe^7H\alpha$ and Asn^8NH (12, 17). A rough estimation (17) of chromophore-proton distances from Johnson-Bovey diagrams qualitatively confirmed the results reported here. These data, calculated from non-NOE measurements, support the D-Phe^7 side chain conformation and the proposed Orn^2 and D-Phe^7 (ϕ, ψ) angles of the β-pleated sheet.

The two possible conformations for the Asn^8 residue, $(\phi, \psi) = (-154°, +170°)$ or (−86°, +170°), deviate slightly from the antiparallel β-pleated sheet conformation but this is consistent with the finding that the Asn^8NH does not form as strong a hydrogen bond (23) (the values of k_{HDX} and $\Delta\delta/\Delta T$ are half-way between those of a hydrogen-bonded and solvent-exposed proton). However, the transannular distances involving the Asn^8NH proton and both the Val^1NH and $Orn^2H\alpha$ support the approximately antiparallel β-pleated sheet conformation.

The β-turn Residues

THE D-PHE^4-PRO^5 RESIDUES The determination that $r[H\alpha(4)\text{-}H\delta1(5)] = r[H\alpha(4)\text{-}H\delta2(5)] = 2.2 \pm 0.1$ Å places $\psi(4) = -130° \pm 15°$. Thus the $(\phi, \psi) = (+66°, -130°)$ angles of D-Phe^4 correspond to those of the second residue of type II′ β-turns (Table IX).

A complete spin-spin analysis of the Pro^5 residue in tyrocidine A gave χ^1, χ^2, and χ^3 (17) and proved unequivocally that Pro^5 has a Ramachandran B conformation $(\phi, \chi^1, \chi^2, \chi^3, \chi^4) = (-70°, +30°, -34°, +30°, +14°)$. The small NOE between $Pro^5H\alpha$ and Phe^6NH and the inefficient relaxation of the $Pro^5H\alpha$ support the contention that the $Pro^5H\alpha$ is a relatively isolated proton and the $r\psi(5) > 3.0$ Å. This value of $r\psi(5)$ corresponds to $\psi(5) = -150°$ to +30° but examination of the (ϕ, ψ) conformational map of N-acetyl-N'-methyl alanine amide (22) shows that the range between −150° and −70° is not allowed. Therefore $\chi(5)$ is limited to the range −70° to +30°. These latter values compare favorably with the (ϕ, ψ) angle and $(r\phi, r\psi)$ distances of a typical type II′ β-turn as shown in Table IX. The D-Phe^4-Pro^5 sequence therefore has a type II′ β-turn conformation, which is confirmed by the hydrogen bonding of the Phe^6NH and solvent exposure of D-Phe^4NH (26).

TABLE IX

DIHEDRAL ANGLES FOR β-TURNS

	ϕ*	$r\phi$	ψ^{i+1*}	$r\psi$	$r(\phi,\psi)$	ϕ*	$r\phi$	ψ^{i+2*}	$r\psi$	$r(\phi,\psi)$
				(Å)	(Å)				(Å)	(Å)
I (LL)	−60°	2.80	−30°	3.53	2.7	−90°	2.92	0°	3.30	2.3
I′ (DD)	+60°	2.80	+30°	3.53	2.7	+90°	2.92	0°	3.30	2.3
II (LL)	−60°	2.80	+120°	2.14	4.7	+80°	2.27	0°	3.30	2.5
(LD)	−60°	2.80	+120°	3.30	4.7	+80°	2.89	0°	3.30	2.5
II′ (DD)	+60°	2.80	−120°	2.14	4.7	−80°	2.27	0°	3.30	2.5
(DL)	+60°	2.80	−120°	3.30	4.7	−80°	2.89	0°	3.30	2.5
III (LL)	−60°	2.80	−30°	3.53	2.7	−60°	2.80	−30°	3.53	2.7
III′ (DD)	+60°	2.80	+30°	3.53	2.7	+60°	2.80	+30°	3.53	2.7
D-Phe^4-Pro^5	+66°	2.8	−130°	—	—	−70°	—	−70~ +30°	>3	—
Gln^9-Tyr^{10}	−73°	2.9	0°	3.3	2.8	−105°	3.0	−25°	3.5	2.4

Comparison of (ϕ, ψ) dihedral angles and ($r\phi$, $r\psi$) distances for the i + 1 and i + 2 residues of common β-turn conformations with those of D-Phe^4-Pro^5 and Gln^9-Tyr^{10} sequences of tyrocidine A. A new criterion of the $r(\phi, \psi)$ distance between amide protons is also included; the latter can be between NH(i + 1) $\leftrightarrow$ NH(i + 2) and NH(i + 2) $\leftrightarrow$ NH(i + 3).

*Typical ϕ, ψ dihedral angles (43) for β-turns.

THE GLN^9-TYR^{10} RESIDUES The sequence Asn^8-Gln^9-Tyr^{10}-Val^1 was proposed to have a type I β-turn rather than a type II β-turn from the $^3J_{NHH\alpha}$ values of Gln^9 and Tyr^{10} residues (26). However, even the determination of [$r\phi(9)$, $r\psi(9)$], [$r\phi(10)$, $r\psi(10)$] angles based upon $^3J_{NHH\alpha}$ values and NOEs indicates the sequence Gln^9-Tyr^{10} can be consistent with 16(ϕ, ψ) combinations and therefore conformations. Thus, information, in addition to $r\phi$, $r\psi$ distances for each residue, is needed for unequivocal determination of the dihedral angles for the $i+1$ and $i+2$ residues in a four residue β-turn sequence.

We have shown that measurement of, say, NH(i)-NH($i+1$) distances removed the fourfold degeneracy of (ϕ, ψ) combinations derived from $r\phi$ and $r\psi$ distance measurements. In this way the number of (ϕ, ψ) combination for Gln^9 is reduced from four to three (Table VII). One of the combinations for the Gln^9-Tyr^{10} sequence, (−73°, −1°) and (−105°, −25°), is consistent with a type I β-turn (Table IX). These (ϕ, ψ) angles are also consistent with the observation that Val^{1}NH is hydrogen bonded (26) and Gln^{9}NH is exposed to the solvent (26). The Tyr^{10}NH should be solvent exposed in this (ϕ, ψ) combination, but it had been postulated that the amide proton was hidden from the solvent by Gln^9 or Tyr^{10} side chains (26).

It is therefore concluded that the Gln^9, Tyr^{10} sequence is part of a type I β-turn.

MOLECULAR DYNAMICS OF TYROCIDINE A The use of σ ratios and NOE ratios to determine $r\phi$, and $r\psi$ distances from the ProHδ methylene distance assumed a similar correlation time for all ϕ, ψ motions along the ring and further, that this correlation time equalled that of the (Hδ1-Hδ2) vector. The agreement between these $r\phi$ distances and $r\psi$-derived directly from scalar coupling constants supported this assumption. Calculation of $r\phi$ and $r\psi$ distances from relaxation data based upon other calibration distances (from $^3J_{NHH\alpha}$) gave the same values as those from the (Hδ1-Hδ2) vector. This again confirmed our hypothesis concerning ϕ and ψ motions along the ring.

The calculation of $\tau_c = 1.3 \times 10^{-9}$ for five (NH-Hα) vectors proved that ϕ motion for these was essentially the same.

This value $\tau_c = 1.3 \times 10^{-9}$ is almost the same as that obtained for gramicidin S from proton (11) and ^{13}C (37, 38) relaxation studies and we propose that it represents the correlation time for molecular reorientation of the tyrocidine A molecule.

The correlation times for three side chains, Pro[5], Asn[8], and Tyr[10], were determined from the appropriate cross-relaxation parameters and side chain interproton vector distances that are independent of motion or conformation. The values were identical to those obtained for the (NH-Hα) backbone vectors. We conclude therefore, that either these side chains are frozen or that their internal rotational frequency is such that their relaxation is dominated by that of the backbone motions.

We are grateful to Doctors N. Niccolai, C. R. Jones, and K. P. Sarathy for helpful discussions.

This work was supported by grants from the National Institutes of Health (AM 18604), the National Science Foundation (BMS 70.23819 and PCM 77.13976), and the College of Agriculture and Life Sciences. Partial expenses for the Bruker WH270 campus facility were provided by the Graduate School Research Committee and the University of Wisconsin Biomedical Research grant RR 07098.

Received for publication 10 January 1979 and in revised form 24 March 1980.

REFERENCES

1. NOGGLE, J. H., and R. E. SCHIRMER. 1971. The Nuclear Overhauser Effect. Academic Press, Inc., New York. Ch. 3, pp. 44–76.
2. CAMPBELL, I. D., and R. FREEMAN, 1973. Influences of cross-relaxation on NMR spin-lattice relaxation times. *J. Magn. Reson.* **11**:143–162.
3. NICCOLAI, N., M. P. L. MILES, S. P. HEHIR, W. A. GIBBONS. 1978. Correlation time measurements of amino acid side chains from ^{1}H selective spin-lattice relaxation ratios. *J. Am. Chem. Soc.* **100**:6258.
4. GIBBONS, W. A., D. CREPEAUX, J. DELAYRE, J. J. DUNAND, G. HADJUKOVIC, and H. R. WYSSBROD. 1975. The study of peptides by INDOR, difference nmr and time-resolved double resonance techniques. *In* Peptides: Chemistry, Structure and Biology. R. Walter and J. Meienhofer, editors. 127–137. Ann Arbor Science.
5. LEACH, S. J., G. NEMETHY, and H. A. SCHERAGA. 1977. Use of proton nuclear Overhauser effects for the determination of conformations of amino acid residues in oligopeptides. *Biochem. Biophys. Res. Commun.* **75**:207–215.
6. RAE, I. D., E. R. STIMSON, and H. A. SCHERAGA. 1977. Nuclear Overhauser effects and the conformation of gramicidin S. *Biochem. Biophys. Res. Commun.* **77**:225–229.
7. KHALED, M. C., and D. W. URRY. 1976. Nuclear Overhauser enhancement demonstration of type II β-turn peptides of tropoelastin. *Biochem. Biophys. Res. Commun.* **70**:485–491.
8. GLICKSON, J. D., S. L. GORDON, T. P. PITNER, D. G. AGRESTI, and R. WALTERS. 1976. Intramolecular ^{1}H nuclear Overhauser effect study of the solution conformation of valinomycin in dimethyl sulfoxide. *Biochemistry.* **15**:5721–5729.
9. JONES, C. R., C. T. SIKAKANA, S. HEHIR, M. KUO, and W. A. GIBBONS. 1978. The quantitation of nuclear Overhauser effect methods for total conformational analysis of peptides in solution—application to gramicidin S. *Biophys. J.* **24**:815–832.
10. JONES, C. R., C. T. SIKAKANA, M. KUO, and W. A. GIBBONS. 1978. Interproton distances for the β-turn residues of the peptide gramicidin S determined from nuclear Overhauser effect ratios. *J. Am. Chem. Soc.* **100**:5960–5961.
11. JONES, C. R., C. T. SIKAKANA, S. P. HEHIR, and W. A. GIBBONS. 1978. Individual residue correlation times of peptides from proton relaxation parameters: application to gramicidin S. *Biochem. Biophys. Res. Commun.* **83**:1380–1387.
12. KUO, M., C. R. JONES, T. H. MAHN, P. R. MILLER, L. J. F. NICHOLLS, J. J. FORD, and W. A. GIBBONS. 1979. Simplification and spin-spin analysis of the side chain proton magnetic resonance spectrum of the decapeptide

gramicidin S using difference scalar decoupling and biosynthesis of specifically-deuterated analogs. *J. Biol. Chem.* **254**:10301–10306.
13. KALK, A., and H. J. C. BERENSEN. 1976. Proton magnetic relaxation and spin diffusion of proteins. *J. Magn. Reson.* **24**:343–366.
14. SYKES, B. D., W. E. HULL, and G. H. SNYDER, 1978. Experimental evidence for the role of cross-relaxation in proton nuclear magnetic resonance spin lattice relaxation time measurements in proteins. *Biophys. J.* **21**:137–145.
15. BALARAM, P. A., A. A. BOTHNER-BY, and E. BRESLOW. 1973. Nuclear magnetic resonance studies of the interactions of peptides with bovine neuroficin. *Biochemistry.* **12**:4695–4704.
16. GIBBONS, W. A., C. F. BEYER, J. DADOK, R. F. SPRECHER, and H. R. WYSSBROD. 1975. Studies of individual amino acid residues of the decapeptide tyrocidine A by proton double-resonance difference spectroscopy in the correlation mode. *Biochemistry.* **14**:420–428.
17. KUO, M., and W. A. GIBBONS. 1979. Determination of side chain and tertiary conformations of tyrocidine A from scalar coupling constants and chemical shifts. *Biochemistry.* **18**:5855–5867.
18. WYSSBROD, H. R., M. FEIN, J. DADOK, R. F. SPRECHER, C. F. BEYER, L. C. CRAIG, P. ZIEGLER, and W. A. GIBBONS. 1973. Tyrocidine A: assignments of the PMR spectrum intramolecular hydrogen bonding and side chain orientations. Abstract of the American Chemical Society National Meeting, Chicago, Ill. 184.
19. BYSTROV, V. F. 1976. Spin-spin coupling and the conformational states of peptide systems. *Prog. NMR Spectroscopy.* **10**:41–81.
20. SOLOMON, I. 1955. Relaxation process in a system of two spins. *Physics Rev.* **99**:559–565.
21. WOESSNER, D. E. 1965. Nuclear magnetic dipole-dipole relaxation in molecules with internal motion. *J. Chem. Phys.* **42**:1855–1859.
22. LEWIS, P. N., F. A. MOMANY, and H. A. SCHERAGA. 1973. Energy parameters in polypeptides. VI. Conformational energy analysis of the *N*-acetyl-*N'*-methyl amides of the twenty naturally occurring amino acids. *Isr. J. Chem.* **11**:121–152.
23. DYGERT, M., N. GO, and H. A. SCHERAGA. 1975. Use of a symmetry condition to compute the conformation of gramicidin S. *Macromolecules.* **8**:750–761.
24. WALTER, R., R. T. HAVRAN, I. L. SCHWARTZ, L. F. JOHNSON. 1971. Interaction of D_2O, Co^{+2}, Ni^{+2} and Cu^{+2} with oxytocin. *In* Proceedings X European Peptide Symposium. E. Scoffone, editor. Abano Terne, Italy, 1969. North-Holland Publishers Co., Amsterdam. 255–265.
25. WALTER, R. 1971. Structure-activity relationships of protein and polypeptide hormones. *Excerpta Med. Int. Congr. Ser.* **241**:181–192.
26. WYSSBROD, H. R., M. FEIN, M. KUO, and W. A. GIBBONS. 1980. Secondary structure and hydrogen bonding of tyrocidine A. *Biochemistry.* In press.
27. FREEMAN, R. H., H. D. W. HILL, B. L. TOMLINSON, and L. D. HALL. 1974. Dipolar contribution of NMR spin-lattice relaxation of protons. *J. Chem. Phys.* **61**:4466–4473.
28. HALL, L. D., and H. D. W. HILL. 1976. Spin-lattice relaxation of protons. A general, quantitative evaluation of contributions from the intramolecular dipole-dipole mechanism. *J. Am. Chem. Soc.* **98**:1269–1270.
29. VOLD, R. L., R. R. VOLD, and D. CANET. 1977. Anisotropic reorientation of planar molecules measured by nuclear relaxation in strongly coupled spin systems. *J. Chem. Phys.* **66**:1202–1216.
30. VOLD, R. L., and R. R. VOLD. 1978. Nuclear magnetic relaxation in coupled spin systems. *Prog. NMR Spectroscopy.* **12**:79–133.
31. LLINÁS, M., M. P. KLEIN, and K. WUTHRICH. 1978. Amide proton spin-lattice relaxation in polypeptides. A field dependence study of the proton and nitrogen dipolar interactions in alumichrome. *Biophys. J.* **24**:849–862.
32. BLEICH, H. E., K. R. K. EASWARN, J. A. GLASEL. 1978. The contributions to amide proton spin-lattice relaxation in small peptides. *J. Magn. Reson.* **31**:517–522.
33. KUO, M., T. DRAKENBERG, and W. A. GIBBONS. 1980. A study of proton relaxation mechanisms, stereochemistry and dynamics of the decapeptide tyrocidine A. *J. Am. Chem. Soc.* **102**:520–524.
34. WERBELOW, L. G., and D. M. GRANT. 1975. Carbon-13 relaxation in multispin systems of the type AX_n. *J. Chem. Phys.* **63**:544–556.
35. NICCOLAI, N., H. K. SCHNOES, W. A. GIBBONS. 1980. The study of stereochemistry, relaxation mechanisms of internal motions of natural products utilizing proton relaxation parameters: the solution and crystal structures of saxitoxin. *J. Am. Chem. Soc.* **102**:1513–1517.
36. HULL, S. E., R. KARLSSON, P. MAIN, M. M. WOOLFSON, and E. J. DODSON. 1978. The crystal structure of a hydrated gramicidin-S-urea complex. *Nature (Lond.).* **275**:206–207.
37. ALLERHAND, A., and R. A. KOMORSKI. 1973. Study of internal rotations in gramicidin S by means of carbon-13 spin-lattice relaxation measurements. *J. Am. Chem. Soc.* **95**:8828–8831.

38. Komorski, R. A., I. R. Peat, and G. C. Levy. 1975. High field carbon-13 NMR spectroscopy: Conformational mobility in gramicidin S and frequency dependence of carbon-13 spin-lattice relaxation times. *Biochem. Biophys. Res. Commun.* **65**:272–279.
39. Sogn, J. A., L. C. Craig, E. W. Randall, and W. A. Gibbons. 1973. The study of nitrogen-15 labeled amino acids and peptides by NMR spectroscopy. *Biochemistry.* **12**:2100–2105.
40. Stern, A., W. A. Gibbons, and L. C. Craig. 1968. A conformational analysis of gramicidin S by nuclear magnetic resonance. *Proc. Natl. Acad. Sci. U.S.A.* **61**:734–741.
41. Ohnishi, M., and D. W. Urry. 1969. Temperature dependence of amide proton chemical shifts: the secondary structures of gramicidin S and valinomycin. *Biochem. Biophys. Res. Commun.* **36**:194–202.
42. Momany, F. A., R. F. McGuire, A. W. Burgess, and H. A. Scheraga. 1975. Energy parameters in polypeptides. VII. Geometric parameters, partial atomic charges, nonbonded interactions, hydrogen bond interactions, and intrinsic torsional potentials for the naturally occurring amino acids. *J. Phys. Chem.* **79**:2361–2381.
43. Venkatachalam, C. M. 1968. Stereochemical criteria for polypeptides and proteins. V. Conformation of a system of three linked peptide units. *Biopolymers.* **6**:1425–1436.